THE UNIVERSITY *of* EDINBURGH
School of Physics
and Astronomy

Constraining the Effective Field Theory of Dark Energy and Modified Gravity in a Limited Parameter Space

MPhys Project Report

S. Smith - s1541136

Submitted for the 40pt MPhys Project course PHYS11016
April 5, 2020

Abstract

The late-time cosmic expansion is one of the most pivotal discoveries in modern physics. This phenomenon and almost all cosmological observations can be explained by the ΛCDM model. However, the required extreme fine-tuning of the vacuum energy within this model has spawned a search for alternative descriptions of the cosmos. This project investigates the effective field theory of dark energy and modified gravity which replaces the cosmological constant with a dynamical vacuum energy scalar field which couples to the metric. More specifically, by constraining its parametrisation to two free properties; the effective Planck mass, M, and the sound speed of the scalar field, c_s. By fitting its predictions to cosmological observations, a present-day value of the Planck mass was found to be $1.11 \leq M_0^2 \leq 1.28$ at a 95% confidence level.

Supervisor: Professor A. Taylor

Personal statement

At the beginning of the academic year, my supervisor informed that the project involved intensive theoretical cosmology. I was provided with and read in-depth lecture slides about dark energy and modified gravity. These slides were my main point of resource for understanding the underlying concepts of the project and were used throughout the whole year. In the initial weeks of the first semester, I reviewed basic cosmology that I had learned in fourth year. This included the ΛCDM model, dark energy as a cosmological constant and its observational evidence, Friedmann equations, and the FRLW metric. I was also provided with papers which contained material directly relevant to the project and the formalism of the equations I would be working with. After this, I studied cosmological perturbation which proved difficult. I wasn't as familiar with this as with previous cosmology and so getting to grips with this took some time. Finally, we discussed modified gravity and dynamical dark energy with current theoretical examples such as quintessence and k-essence. We also discussed Horndeski gravity and how a general theory of unified gravity could be formed into an effective field theory with the addition of a dynamical scalar field which coupled to the metric. Again, these topics were very conceptually challenging and took time to understand. This background reading accounted for half of the first semester and my supervisor and I met weekly to discuss these topics until I was comfortable with the framework.

I began writing code in week five while I was still researching. I wrote the code in `python` as I was familiar with this language from previous courses I had taken. I first changed the differential variable of the matter density perturbation equation from time to the logarithm of the cosmic scale factor as this would be more useful to use. I then attempted to replicate the density perturbations for Einstein de-Sitter and ΛCDM models. After some tweaking and consultation with my supervisor, I started getting sensible results. We moved onto implementing the modified gravity parameter μ and how it, as well as the vacuum energy equation of state, w, affects the evolution of density perturbations. Once this was working correctly we moved onto parametrising μ in terms of the effective Planck mass, the sound speed of the vacuum energy scalar field as well as the braiding of the scalar field with the metric. This introduced new abstract cosmology which proved difficult and involved large derivations which resulted in a lot of mistakes. As I coded my derivations, the results were diverging and it was hard to identify the problem. Eventually, after speaking with my supervisor, the mistakes were ratified and the code was working. In the final week of the semester, I redefined the braiding parameter in terms of the sound speed into a differential equation. This required further numerical integration which caused more problems and infinities arose. However, December exams were approaching and I put the project aside.

I attempted to fix the code over the Christmas break but unfortunately, I was unsuccessful. Instead, I began planning and writing some background for the report. In our first meeting back in semester two, my supervisor advised me that the code was likely suffering from a numerical error as some parameters approached zero and caused divergences. This was the problem and a small constant was added to one of the parameters and the code started producing sensible results. I submitted what I wrote in my report to my supervisor for feedback. Unfortunately, I had started my report with too much basic background theory

that needed to be removed. Despite this, it wasn't too much of a set back as I had started working on it ahead of time. We then moved onto gravitational potential perturbations and I attempted to reparameterise the equations for the framework of the project. This lead to complex derivations and again resulted in divergences. However, my supervisor realised that there was a simpler route to take. This worked fine but I later realised that I had derived something incorrectly from semester one which was causing problems throughout the code. As I continued to write my theory for the report I noticed where I had gone wrong and then the code became fully functional.

In the latter half of the semester, I was then instructed to use cosmic microwave background data to fit with the theory predictions with a χ^2 test. After my supervisor and I fixed the issue of normalisation of my perturbations, I was able to get results. Furthermore, I compared the predictions to large scale structure data to further constrain my results and this was successful. I then spent the rest of the semester writing my report. However, due to the COVID-19 outbreak, I was unable to communicate with my supervisor as frequently. This, as well as the outbreak itself, slowed progress drastically.

Acknowledgments

I would like to express my utmost gratitude to my supervisor Andy Taylor for his patience and for the time he devoted to assisting me with every aspect of the project.

I would like to thank Bob Man and John Peacock for their well constructed, clear and concise Cosmology course notes. They were of great value to me for understanding the underlying principles of cosmology and they set the foundation of knowledge required for this project.

I would like to thank Ken Rice, Annette Ferguson and Ross McLure for their excellent Astrophysics course notes. These were of great help for Section 2 of the report.

Contents

1 Introduction

One of the greatest and highly pursued puzzles of modern cosmology is the late-time acceleration of the universe. In 1998, it was discovered that the universe was not only expanding but at an ever-increasing rate [1, 2]. Additionally, this accelerating expansion was found to have initiated about 4 billion years ago, as the universe became vacuum dominated [3]. This discovery was key in constraining popular cosmological models to favour flat-Λ Cold Dark Matter (ΛCDM). Here Λ accounts for the majority of the mass-energy density budget of the universe under a cosmological constant; which is a product of Einstein's theory of general relativity (GR). The cosmological constant is responsible for the late-time acceleration in the ΛCDM model by attributing it to the vacuum or dark energy (DE). Today, ΛCDM is regarded as the most successful cosmological model and is referred to as the standard model of cosmology. It accurately describes the evolution of the universe and can account for important observable properties such as the cosmic microwave background (CMB) and the large-scale structure (LSS) of the universe.

Despite the success of ΛCDM, it is still encumbered with the conundrums of dark matter and dark energy which constitutes 95% of the universe's contents. The ΛCDM model incorporates these sources of mass-energy density, but it doesn't explain what they are. Additionally, the model relies on scrupulous fine-tuning to explain certain observable properties of the cosmos. The observational value of the vacuum energy appears to be a factor of the order $\sim 10^{60}$ smaller than the theoretical prediction given by quantum field theory (QFT) [4]. This requires Λ to be accurate to 60 decimal places constituting the so-called 'Cosmological Constant Problem' (CCP). This is one of the biggest discrepancies in the history of physics and marks the colossal chasm between its two most successful theories, GR and QFT. Moreover, ΛCDM has come under scrutiny for its alleged issue of systematic coincidence which may render the model flawed. Despite this, there is an absence of explicit evidence to discard ΛCDM and it remains our best effort to describe the dynamics of the universe. Nevertheless, in the advent of progressively stringent dark energy parameters from future deep-space surveys, it is constructive and of great interest to consider alternative measures to explain cosmic acceleration.

To explore this paradigm, two main approaches have emerged: theories of modified gravity (MG) and dynamical dark energies. The former seeks to solve ΛCDM issues by considering alternative dynamics of GR exclusively. Additionally, cosmologists have developed MG theories which can account for late-time acceleration in its own right [5]. However, it is abundantly clear that GR is exceptionally accurate on local scales and has passed all rigorous testing in the Solar System [6]. Therefore, any developments that diverge from current theories at cosmological scales, must still replicate current GR results locally. Conversely, the CCP has been tackled under the proposition that a DE scalar field may permeate the universe in place of the cosmological constant. The nature of this approach is inextricably linked with particle physics. The natural occurrence of scalar fields in particle physics constitutes a suitable substitute candidate for the form of the vacuum energy. This approach has already been substantially researched by cosmologists over the past two decades [7]. Consequently, this has spawned a plethora of vacuum energy models which attempt to accommodate the shortcomings of ΛCDM [8].

The fundamental source of the present acceleration of the Universe is very poorly understood. This lack of constraint has allowed a vast scope of models to develop which is impossible to test in its entirety. Given this, it seems that concentrating on a more general theoretical approach and constraining it with rigid observable evidence, is a more practical strategy. As there is no particular reason to favour either MG or a variable DE, the logical approach would be to unite the frameworks into a single generalised model. Again, this premise has received extensive investigation which has subsequently prompted an effective field theory (EFT) of MG and DE or unified gravity (UG) [9–11]. Currently, the formalism of the EFT is still in development and is encumbered with some instabilities and inadequate parameterisation of intuitive physical properties of gravity and DE. This has motivated research into the stability of this EFT and whether it is a suitable candidate for the vacuum energy problem [12, 13]. Further work has attempted to avoid instabilities in the EFT [14] by embedding it in Horndeski action [15]. This allows a dynamical DE scalar field to couple with the gravitational metric, to be described by stable second-order equations of motion.

This project is an attempt to build upon this work by reparameterising the free equations of UG in concordance with Horndeski theory (as given in Refs. [16–18]). More specifically, to describe these equations in terms of intuitive physical quantities, namely, the effective Planck mass, M, and the sound speed of the scalar field, c_s. Moreover, this project investigates cosmological perturbations of the matter density and the gravitational potential field in this regime. Subsequently, the theoretical predictions of the LSS growth rate and temperature fluctuations of the CMB are explored under the jurisdiction of M^2 and c_s^2. Lastly, these predictions are compared to observational data of galactic clustering and the power spectrum of the CMB to identify the best-fit present-day parameter values M_0^2 and $c_{s,0}^2$. Consequently, this may lead to values which deviate from the ΛCDM model. Additionally, this will test whether the current formalism of the EFT of UG can produce consistent results.

This report is organised as follows. Section 2 outlines the fundamentals of the cosmological constant, its observational evidence and discusses the shortcomings of ΛCDM. Section 3 is concerned with the underlying work and theory that is related to the project. More specifically, Horndseski gravity, the EFT of UG and modified cosmological perturbation theory. Section 4 discusses the methods used to specify UG in terms of M^2 and c_s^2, the numerical methods used to solve the modified perturbation equations and how these predictions were compared to the CMB and LSS to constrain the present-day values. The results of the project are analysed in section 5. Section 6 briefly discusses possible areas of progression. Finally, section 7 aims to give a final statement of the main concerns and outcome of the project.

2 The Cosmological Constant

2.1 Interpretation

The cosmological constant is a homogeneous energy density that causes the expansion of the universe to accelerate. It was originally introduced by Albert Einstein in 1917 [19] to allow a

static universe solution. This can be explained by considering Poisson's equation of Newton's gravitational potential, $\nabla^2\Psi = 4\pi G_N \rho$. Where G_N denotes Newton's gravitational constant. Einstein proposed that if the density of the universe, ρ, is constant (as it was thought to be), then so should the gravitational potential, Ψ [20]. This required an additional term to counter gravitational attraction,

$$\nabla^2\Psi = 4\pi G_N \rho - \Lambda. \tag{1}$$

Here Λ is a cosmological constant that is thought to be an intrinsic part of the vacuum. For the universe to be static, Λ would cancel with gravity which prevents any acceleration ($a = -\nabla\Psi = 0$). This introduces an odd concept where it is required that Λ is a source of negative pressure, $p_\Lambda = -\rho_\Lambda c^2$. It was subsequently abandoned when the universe was found to be expanding. Now, the cosmological constant is invoked to explain the observed acceleration of the expansion of the universe. This favoured ΛCDM which predicts its equation of state to be $w \equiv p_\Lambda/\rho_\Lambda = -1$ (natural units). This prediction was confirmed by the *Planck* mission which found $w = -1.03 \pm 0.03$ [21]. Thus, Λ is considered the prime candidate as it can account for this repulsive force opposing gravity.

Its existence is also predicted by quantum physics, where it enters as a form of vacuum energy which is responsible for particle pair production. However, there is a colossal discrepancy between observational and theoretical values. It may seem that Λ represents an unlimited source of energy, as its value remains constant even after expansion. However, the work done to expand the universe is exactly replaced by the intrinsic vacuum energy of the larger, expanded space. This dynamic allows Λ to remain constant. Unfortunately, the source of this energy is still unknown and is labelled 'dark energy' but is predicted to constitute $\sim$70% of the mass-energy density budget of the universe. Despite the abstract and seemingly contrived nature of Λ, this is an extremely well-founded physical prediction. The ΛCDM model can account for every piece of observational data to date and the existence of Λ is firmly supported by various independent cosmological observations.

2.2 Observational Evidence

2.2.1 Supernovae

The original compelling piece of evidence of an accelerating universe came in 1998. Two independent teams arrived at this conclusion by observing type Ia supernovae (SN Ia) [1,2]. A supernova is a catastrophic explosion of a massive star that occurs at the end of its life. When nuclear fusion is exhausted in a star's core, the only mechanism to counter its gravitational collapse is the electron degeneracy pressure (EDP) of the inert matter in the core. This is known as a *white dwarf*. However, if a star exceeds the limit of 1.44 $M_\odot$ — Chandrasekhar limit, EDP can no longer sustain the star's gravitational collapse. Subsequently, β^+-decay occurs and the structure becomes a neutron star. This causes a sudden collapse which results in a colossal shock-wave that expels radiation and the star's outer contents into

space. These events are extremely bright and can outshine galaxies. Type 1a refers to a binary system of stars where one is a white dwarf. Furthermore, SN Ia exhibit unique spectral lines making them easily identifiable. The white dwarf accretes mass from its companion until it reaches the Chandrasekhar limit and creates a supernova. Because SN Ia occur when the star is exactly 1.44 $M_\odot$, the maximum *absolute magnitude* (intrinsic brightness), M, of their supernovae, are consistent throughout time and space. This unique property of SN Ia grants them the label of *standard candle*. This property is extremely useful for determining the distance to these events. In reality, things are more complicated as there is too large a variance of the absolute magnitudes to produce precise cosmological constraints. However, at the end of the 1990s, astronomers were able to identify a relationship between the absolute magnitude and the width of the light curve [22]. This relationship permits the determination of the supernovae absolute magnitude or intrinsic luminosity and thus, can be used as standard candles. By measuring the apparent magnitude, m, of an SN Ia, the luminosity distance, d_L, can be determined,

$$m - M = 5\log_{10}\left(\frac{d_L}{\text{Mpc}}\right) + 25. \tag{2}$$

Additionally, the distance to bright bodies can be calculated by considering their redshift, z. The distance to redshift relation is dependent on the contents of the universe which are in turn a function of z. In a universe dominated by matter and DE with a negligible radiation energy density, $\Omega_r \simeq 0$; the distance-redshift relation can be derived from the Friedman equations [23] and is given by,

$$d_L = \frac{c(1+z)}{H_0}\int_0^z \left(\Omega_m(1+z')^3 + \Omega_v(1+z')^{-3(1+w)} + \Omega_k(1+z')^2\right)^{-\frac{1}{2}} dz'. \tag{3}$$

Where the density parameters $\Omega_i \equiv \rho_i/\rho_c$, ρ_c is the critical density of the universe and $i = m, v, k$ for matter, vacuum and curvature, respectively. H_0 is the present day Hubble factor, c is the speed of light in a vacuum and w is the equation of state of DE. Under the flat ΛCDM model, we have $\Omega_k = 0$ ($\Omega_0 = 1$)[1] and $w = -1$ and thus, $\Omega_v \to \Omega_\Lambda$. Subsequently,

$$d_L = \frac{c(1+z)}{H_0}\int_0^z \left(\Omega_m(1+z')^3 + \Omega_\Lambda\right)^{-\frac{1}{2}} dz'. \tag{4}$$

As one would expect, if $\Omega_\Lambda = 0$, then a there would be a linear relation between M and $\log(z)$. However, the SN Ia data conveyed that supernovae were appearing less bright than expected at increasing distances. Consequently, the data exhibited a divergence from this linear relation at large z. This phenomenon could be accounted for at all z if $\Omega_\Lambda \simeq 0.7$. This reintroduced Λ to mainstream cosmology. Some years later, additional SN Ia data reasserted the requirement for a cosmological constant [24, 25]. Of course it is possible that $w \neq -1$ and another solution exists for Ω_v and this lead to work on determining $w(z)$ with SN Ia data [26] and more recently [27]. The large uncertainties on SN Ia data meant that the equation of state couldn't be significantly constrained but still favoured $w = -1$.

[1] Ω_0 refers to the total present day density parameter

2.2.2 Large Scale Structure

Observations of the LSS such as galaxy clustering can further indicate a requirement for dark energy. The matter power spectrum, $P(k)$, describes the variance of density from the average at different scales or Fourier modes, k. On large scales, where only gravity and cosmic expansion are prevalent, structure grows linearly and $P \propto \ln k$. On smaller scales, other mechanisms become important such as virialisation and consequently, there is a turnover of P and it starts to decrease. Naturally, the peak of the power spectrum is dependent on Ω_m. Smaller values of Ω_m correspond to a peak at larger scales or smaller k. The presence of dark energy, therefore, favours a peak at larger scales.

The measurable galaxy power spectrum is related to the matter power spectrum via a bias parameter, b,

$$P_g(k) = b^2 P(k). \tag{5}$$

This parameter simply sets the amplitude of $P(k)$. From a variety of surveys including *Planck*, the galaxy power spectrum exhibits a peak that matches the ΛCDM prediction. Galaxies are sufficiently small that other mechanisms need to be considered when describing the power spectrum at these scales. Consequently, the physics behind b isn't well defined. This means that tight constraints on Ω_Λ can't be determined from this method. Nevertheless, due to the position of the peak, the galactic power spectrum favours a model with a significant vacuum energy.

2.2.3 Cosmic Microwave Background

The existence of dark energy is further reinforced by the CMB. The CMB is a remnant of the big bang which can be seen in all directions in space. Up until the universe was ~ 400 kyr old, baryonic matter was completely ionised due to the extremely hot and dense state. At this epoch, radiation was a significant constituent of the mass-energy density budget which comprised a photon-baryon fluid. This fluid underwent Thompson scattering meaning the photons had a very small mean-free-path and consequently, the early universe was opaque. When the universe expanded and cooled, electrons and nuclei formed atoms. The photons were redshifted under cosmic expansion and became insufficiently energetic to ionise the atoms. This meant that the photons had *decoupled* from matter and the universe became transparent. This relic radiation is known as the CMB which provides a 'snapshot' of the *last scattering* the photons experienced at this epoch. Thus, any features of the CMB allows us to infer properties of the universe at last scattering. Conversely, the vacuum energy is believed to have been negligible at this epoch and so the CMB is unable to provide evidence for it directly. Despite this, the CMB has proved to be one of the greatest probes for constraining cosmological parameters, that a significant vacuum energy can be invoked.

Initial partial-sky surveys such as BOOMERang [28] and MAXIMA [29] gave indications that the universe was flat. However, it wasn't until 2001 the *Wilkinson Microwave Anisotropy*

Probe (WMAP) was launched and supplied data from which a precise CMB power spectrum was developed [30] (see Fig. 1 for *Planck* spectrum). This spectrum contains a variety of features that aided in constraining multiple cosmological parameters. The first and largest peak of the CMB power spectrum corresponds to scalar perturbations that can infer the curvature of the universe. The ninth and final data release showed that the universe is exceptionally flat $\Omega_k = -0.0027 \pm 0.00385$ [30]. Moreover, the *Planck* mission constrained this parameter even further, $\Omega_k = 0.001 \pm 0.002$, reinforcing the result. Partnering this with other independent measures of $\Omega_m \simeq 0.3$ from the LSS shows that there is a large constituent of the energy-density budget that is unaccounted for, $\Omega_x = 1 - \Omega_m$. Reproducing the CMB power spectrum from ΛCDM matches the observed data extremely accurately.

2.2.4 Age of the Universe

It should be stated, that even before conclusive evidence of acceleration was found, cosmologists already had a motive for some substance responsible for cosmic acceleration. This postulation emerged due to the comparison of the theoretical age of the universe and the ages of the oldest stellar populations. The development of inflationary theory succeeded in accounting for cosmological conundrums [31] and gained popularity in the early 80s. Inflation predicts a late-time flat universe and subsequently, this became a favoured feature of cosmological models. Despite this, in the early 90s, measurements of the matter density were falling significantly short of the necessary amount: $\Omega_m \sim 0.3$ [32]. With $H_0 \approx 70$ km s^{-1} Mpc^{-1} as the current value of the Hubble factor, the theoretical age of an open universe is calculated to be ∼11.3 billion years old [2]. Conversely, estimations of the age of the oldest galaxy clusters were found to be (13.5 ± 2) billion years [33]. Moreover, the discovery of massive galactic clusters at $z = 1$ [34], independently strongly suggested that $\Omega_m < 1$. The discrepancy of theoretical and observational ages of the universe can be reduced to a negligible difference by introducing a new source of energy density such that the universe is flat. Although this discrepancy doesn't predict the vacuum energy specifically, it does, however, suggest that a significant constituent was being unaccounted for. With the discovery of cosmic acceleration in 1998, the cosmological constant resolved the age disparity now predicting 13.8 billion years which is consistent with all observations to date.

2.2.5 Present Day Results

All of the above tests of dark energy has allowed its parameters to be constrained to a precise degree. There have been various additional methods to probe dark energy and its properties, such as baryon acoustic oscillations [35]. The results of the recent *Planck* data release of the CMB power spectrum, have been constrained in conjunction with these experiments to give the latest and best fit cosmological parameters. These include the relevant dark energy parameters,

[2] At the time $H_0 = 80$ km s^{-1} Mpc^{-1} [32] which results in an even lower age for the universe.

$$\Omega_\Lambda = 0.6889 \pm 0.0056$$
$$w = -1.03 \pm 0.03$$

.

2.3 Problems with the Cosmological Constant

2.3.1 Cosmoligical Constant Problem

Despite the successes of the ΛCDM model, it still posses some critical issues. Firstly, is the colossal discrepancy between the theoretical quantum prediction of the vacuum energy and its observed value [36]. To understand this, the origin of Λ and the expected quantum mechanical value of the vacuum density need to be considered.

GR allows for an intrinsic cosmological constant as discussed in Sec. 2.1. In a purely classical framework, this constant could take any value as it is just a fundamental parameter of GR. This 'bare' cosmological constant, Λ_b, cannot be predicted by the theory and only constrained by observation. Introducing a quantum description, QFT tells us that the vacuum has a non-zero energy ground state. Therefore, in the absence of matter or radiation, the zero-point energy density can be given as,

$$\langle 0|\rho(\vec{x},t)|0\rangle = \rho_v. \tag{6}$$

From isotropy and homogeneity, the vacuum state should be the same for each observer. Subsequently, from continuity ρ_v is constant. This is the same phenomenon as with Λ_b and thus an effective cosmological constant can be given as,

$$\Lambda \equiv \Lambda_b + 8\pi G_N \rho_v. \tag{7}$$

To obtain a full description of ρ_v a theory of quantum gravity is required. However, a semi-classical formalism can be applied as given in Ref. [36],

$$\rho_v = \sum_i (-1)^{2s_i} \frac{n_i m_i^4}{64\pi^2} \ln\left(\frac{m_i^2}{\mu^2}\right). \tag{8}$$

This describes a summation over the fundamental quantum fields of the standard model where, m, is the mass, s, is intrinsic spin, n, is the number of degrees of freedom and μ is the renormalisation energy-scale used to prevent divergences. This gives a QFT vacuum energy of [37],

$$|\rho_v| \sim 10^8 \text{ GeV}^4. \tag{9}$$

Conversely, the energy density of the cosmological constant can be calculated by rearranging the Friedman equation for the critical density and multiplying by Ω_Λ,

$$\rho_\Lambda = \Omega_\Lambda \rho_{c,0} = \Omega_\Lambda \frac{3H_0^2}{8\pi G} \sim 10^{-47} \text{ GeV}^4 \tag{10}$$

There is a huge difference between the QFT and ΛCDM value for the vacuum energy which is about 55 orders of magnitude. This would mean that Λ_b would need to be accurate to 55 decimal places which constitutes extreme fine-tuning. This is known as the Cosmological Constant Problem and is an extremely active topic of research over the past two decades [4, 18, 38]. Additionally, see Refs. [36, 39] for a more comprehensive analysis.

2.3.2 Coincidence Problem

The cosmological constant is intriguing as Λ remains constant whereas matter and radiation become more dilute as the universe expands. Therefore, it was inevitable that the vacuum would become dominant at some point. However, why is the universe becoming vacuum dominated now? Both the matter and vacuum density parameters are of similar values today and are the same order of magnitude. This appears to place us in an exceptionally 'special' point in the universe's life. In other words, for the vast majority of the universe's lifetime, beforehand and in the future, it will be dominated by one source of mass-energy density by several orders of magnitude. This puts us in an extremely rare epoch and has constituted the so-called 'coincidence problem' [37, 40]. Despite this, there is no particular physical reason as to why this should not be occurring, only its statistical significance. Nevertheless, this fine-tuning still calls the ΛCDM model into question; is this a coincidence? Or is the model flawed?

3 Dark Energy & Modified Gravity

3.1 Methodology

The required fine-tuning of parameters within the concordance cosmology has motivated a search beyond the ΛCDM model. The simplest non-trivial modification is to introduce a new scalar field, $\phi(x,t)$, which represents a dynamical vacuum energy that couples to the metric tensor or gravity. The motivation behind a scalar field comes from their natural occurrence in particle physics. This includes but is not limited to, the Higgs field. The discovery of the Higgs boson and with it, the existence of a fundamental scalar field, justifies the proposition of a DE field as a prime candidate to replace the cosmological constant. However, this raises

the issue of complete freedom to choose the form of ϕ. The dynamics and the form of its potential are entirely unknown meaning its Lagrangian could be a wide range of options. As previously discussed, this has lead to a vast scope of models which are hypothesised under contrived Lagrangians. Alternatively, in the interest of remaining general, the formalism of the Lagrangian may be constrained under reasonable assertions. Firstly, it is necessary that the Lagrangian is inheritably stable and avoids divergences. Therefore, it can be stated that the Lagrangian must only produce, at most, second-order differential equations of motion. This is because higher-order Lagrangians result in Ostrogradski instabilities which are diverging energy levels [41]. This can be implemented with Horndeski theory (see Sec. 3.2). As illustrated below, the Horndeski Lagrangian is exceptionally complex in its entirety and thus, it is constructive to further constrain the theory. This can be applied with little loss of generality to create an EFT of UG. From here, UG can be parameterised by the Planck mass, M, and the sound speed of the scalar field, c_s. Here, $M^2 \equiv 1/8\pi G_N$ where G_N is Newton's gravitational constant. Therefore, a variable $M^2(a)$ can be thought of as a proxy for the strength of gravity. Henceforth $M^2 \equiv M^2(a)$ and will be quoted in units of $1/8\pi G_N$. Under this parameterisation a generalised EFT of UG can be entirely described by two parameters. This is a simple but powerful tool that can be used to identify any parameter deviations from concordance cosmology and identify if it predicts consistent results.

3.2 Horndeski Gravity

Horndeski theory is the most general Lorentz covariant, four-dimensional theory of gravity described by the metric tensor and a scalar field that provides at most second-order equations of motion [15]. This theory contains Einstein's GR as well as more exotic MG and DE theories such as Brans-Dicke theory [42] and Quintessence [43]. These theories are the simplest MG and dynamical vacuum energy models, respectively. Despite Horndeski theory being developed in 1974, it fell out of use until it was rediscovered in 2011 [44]. This was recognised as a very powerful tool as it offered an alternative approach to MG and DE. This being to constrain the wide range of possible MG and DE models through observational constraint rather than attempting to guess their form; such as Brans-Dicke and Quintessence. Subsequently, an abundance of theoretical Horndeski research [14, 18] and attempts to constrain its models with small scale astrophysical and large scale cosmological observations [45, 46]. For an in-depth review of Horndeski gravity see Ref. [47].

The Horndeski Lagrangian is given by,

$$\begin{aligned}\mathcal{L}_H = {} & G_4 R + G_3 \Box\phi + G_2 + 2G_{4X}\left((\Box\phi)^2 - (\nabla^\mu\nabla^\nu\phi)^2\right) + G_5 G_{\mu\nu}\nabla^\mu\nabla^\nu\phi \\ & - \frac{1}{6}G_{5X}\left((\Box\phi)^3 - 3\Box\phi(\nabla^\mu\nabla^\nu\phi)^2 + 2(\nabla^\mu\nabla^\nu\phi)^3\right)\end{aligned} \tag{11}$$

Where R is the Ricci scalar from Einstein's GR, $X \equiv -\frac{1}{2}\partial_\mu\phi\partial^\mu\phi$ the effective kinetic energy of the scalar field and G_i are arbitrary functions of ϕ and X. GR is recovered when $G_i = 0\ \forall i$

where $i \neq 4$ and $G_4 = 1$. Further examples are Brans-Dicke which is similar to GR but $G_4 = \phi$ and the G_{4X} term remains to avoid instabilities, and Quintessence which again similar to GR but $G_2 = X - V(\phi)$ where V is the potential energy of the scalar field. By considering the modifications of these theories, it is clear that Brans-Dicke is a theory of MG as this directly effects R and therefore the strength of gravity. This effectively changes $G_N \to G_N(x,t)$ and allows deviations from GR. Similarly, Quintessence introduces a scalar field that represents a dynamical DE with kinetic and potential energy terms that don't directly couple to gravity. Horndeski offers many more complex models [8] which allows ϕ to describe the vacuum energy while directly coupling to the metric. Horndeski in its full form is rather complex and difficult to work with, however, reasonable simplifications of the theory can allow an EFT of UG to be formed.

3.3 Effective Field Theory of Unified Gravity

An EFT aims to describe physical phenomena in a particular regime; an example being Newtonian gravity. This theory is exceptionally accurate at specific scales and is more than sufficient for describing gravity on human scales. This can also be said for GR and QFT which suffer singularities and divergences at when applied to Planck energy scales but are otherwise extremely successful. Thus, it is possible to fit Horndeski gravity to the specific regime at hand and contract its Lagrangian down to a more practical theory. In this project, the concerned regime is of low energy sub-horizon cosmological scales which consequently only considers gravity and DE and disregards complex non-linear mechanisms.

Firstly, the FLRW metric can be applied to the theory. Thus, homogeneity and isotropy can be asserted which removes higher-order terms in the Lagrangian. Moreover, all evidence suggests that the curvature of the universe is negligible on sub-horizon scales and thus a flat universe can be assumed. To first order, this produces a very simple Lagrangian which only consists of three terms, however, this only describes background cosmology [18]. Therefore, it is necessary to calculate second-order terms to obtain cosmological perturbation equations. This can be done by considering the perturbed FLRW metric. This describes scalar perturbations of the metric which excludes vector and tensor (gravitational waves) perturbations which are negligible or unnecessary in this framework. The amplitudes of these perturbations can be transformed in the Newtonian gauge such that they are independent of coordinate system [18]. This perturbed metric includes the perturbed Newtonian gravitational potential, Ψ, similar to Eq. 1,

$$d\tau^2 = (1 + 2\Psi)dt^2 - a^2(t)(1 - 2\Phi)\delta_{ij}dx^i dx^j, \tag{12}$$

Here $c = 1$ has been adopted and throughout the remainder of the project. In Einstein's GR, $\Phi = \Psi$. Instead, UG remains general and allows for *anisotropic stress* (see Sec. 3.4) and consequently, we have two gravitational field perturbations Ψ and Φ which describe time dilation and spatial distortion, respectively. From this, second-order Lagrangian terms can be calculated. The derivation of the EFT of UG requires a working knowledge of gauge theory

and GR, consequently, mathematical details are omitted here. However, the Lagrangian is cast into a unitary gauge which absorbs spatial perturbations. This produces a Lagrangian that is only a function of time [18],

$$\mathcal{L}_{UG} = \Omega(t)R - 2\Lambda(t) - \Gamma(t)\delta g^{00} + M_2^4(t)(\delta g^{00})^2 - \bar{M}_1^3(t)\delta g^{00}\delta K_\mu^\mu. \tag{13}$$

Comparing this to Eq. 11, we have $G_4(t) = \Omega(t)$ which dictates the strength of gravity, $\Lambda(t)$ is the cosmological 'constant' which is now permitted to vary with time and $\Gamma(t)$ describes the kinetic dynamics of the scalar field. Furthermore, δg^{00} is the temporal perturbation of the metric, $M_2^4(t)$ is responsible for non-canonical kinetic behaviour is most notably a feature of k-essence [48]. $\bar{M}_1^3(t)$ allows more exotic kinetic behaviour such as braiding of scalar and tensor terms [49] and $\delta K_{\mu\nu}$ is the perturbation of extrinsic curvature. This is a remarkably simple result and still allows for a large scope of models at the expense of very little generality. Conversely, the constituents of the Lagrangian are unintuitive and can be difficult to test and constrain for this reason. Additionally, deriving perturbation equations from this Lagrangian would be a colossal task. Thus, it is useful to redefine the parameters.

Initially, the effective Planck mass, $M^2 \equiv \Omega(t)$, can be defined. This represents the strength of gravity for perturbation growth. Also, an array of α parameters are defined with subscripts representing their description. These are M — the evolution of the effective Planck mass, K — the kinecticity which is the kinetic energy of the scalar field, and B — the kinetic braiding with the metric.

$$\alpha_M \equiv \frac{(M^2)'}{M^2} \tag{14}$$

$$\alpha_K \equiv \frac{\Gamma + 4M_2^4}{H^2M^2} \tag{15}$$

$$\alpha_B \equiv \frac{H\Omega' + \bar{M}_1^3}{2HM^2} \tag{16}$$

Where H is the Hubble factor and primes represent derivatives with respect to $\ln a$ and henceforth. To recover ΛCDM, $M^2 = 1$ and $\alpha_i = 0\ \forall i$. Finally, we have an EFT of UG which can be described by just six free functions of time: $\Omega, \Lambda, \Gamma, M^2, \alpha_K$ and α_B.

3.4 Cosmological Perturbations

3.4.1 Newtonian Description

The derivations of the perturbation equations in this modified cosmological model are exceptionally cumbersome and again are omitted. Nevertheless, the density perturbation equations can be derived in a Newtonian fashion in the ΛCDM model and subsequently a modification can be invoked from UG. The Newtonian derivation serves as an approximation of the GR

description but is completely sufficient for the concerned regime. We have an expanding universe that can be decomposed into a proper and comoving position,

$$\vec{x}(t) = a(t)\vec{r}(t). \tag{17}$$

Differentiating this twice and substituting in for $r(t)$ from Eq. 17 gives,

$$\ddot{\vec{x}} = \frac{\ddot{a}}{a}\vec{x} + 2\dot{a}\vec{u} + a\dot{\vec{u}}, \tag{18}$$

where $\vec{u}(t) \equiv \dot{\vec{r}}(t)$. The terms with $\vec{u}$ or its derivatives can be attributed to peculiar accelerations, $\ddot{\vec{x}}_p$, and the first term describes the background expansion, $\ddot{\vec{x}}_b$. By only considering peculiar accelerations which occur due to gravitational forces from surrounding matter, $\ddot{\vec{x}}_p = -\nabla\Psi/a$, where a ensures comoving coordinates,

$$2H\vec{u} + \dot{\vec{u}} = -\nabla\Psi/a^2. \tag{19}$$

Where each term has been divided by a and $H \equiv \dot{a}/a$. The continuity equation in comoving coordinates is $\dot{\rho} = -\nabla \cdot (\rho\vec{u})$. Using $\rho = \bar{\rho}(1+\delta)$ where $\bar{\rho}$ is the average density of the universe and δ is a density perturbation,

$$\dot{\delta} = -\nabla \cdot [(1+\delta)\vec{u}], \tag{20}$$

as $\bar{\rho}$ is constant in comoving coordinates. As the framework of this project is only concerned with linear gravitational effects, $\delta \ll 1$ and we have,

$$\dot{\delta} = -\nabla \cdot \vec{u}. \tag{21}$$

Taking the divergence of Eq. 19 and subbing in $\nabla^2\Psi = -4\pi G_N \rho_m a^2 \delta$ from the comoving perturbed Poisson's equation gives the equation of motion for linear density perturbations,

$$\ddot{\delta} + 2H\dot{\delta} = 4\pi G_N \rho_m \delta. \tag{22}$$

3.4.2 Modified Equations

Over the past two decades, a rigorous theoretical effort has provided modified perturbation equations which incorporates all the physics of UG as outlined in Sec. 3.3. Here this modification is invoked from Refs. [50,51] which gives a modified Poisson and shear equation,

$$\nabla^2\Psi = -4\pi G_N \mu(a,k)\rho_m a^2\delta, \tag{23}$$

$$\Phi = \gamma(a,k)\Psi. \tag{24}$$

Here k is the Fourier space wavenumber and imposes a scale dependence on μ and γ. However, Ref. [51] shows that this dependence can be removed for the scales concerned and consequently are only a function of a. Here γ is the effective anisotropic stress which allows for inhomogeneous metric perturbations and μ is an alteration of the strength of gravity in perturbation growth. ΛCDM is recovered for $\mu = \gamma = 1$. These parameters are a product of the Lagrangian given in Eq. 13 and are given as,

$$\mu(a) = \frac{1}{M^2}\frac{2(\alpha_B - \alpha_M)^2 + \alpha c_s^2}{\alpha c_s^2}, \tag{25}$$

$$\gamma(a) = \frac{2\alpha_B(\alpha_B - \alpha_M) + \alpha c_s^2}{2(\alpha_B - \alpha_M)^2 + \alpha c_s^2}. \tag{26}$$

Where all parameters are functions of a, $\alpha \equiv 6\alpha_B^2 + \alpha_K$ and c_s^2 is the sound speed of the scalar field and is described as,

$$\alpha c_s^2 = -2\left(\alpha_B' + (1+\alpha_B)^2 - (1+\alpha_B)\left(1 + \alpha_M - \frac{H'}{H}\right) + \frac{\rho_m}{2H^2M^2}\right). \tag{27}$$

It should be noted that the EFT is only stable if the following restrictions are applied [50],

$$\alpha \geq 0,\ M^2 > 0,\ c_s^2 > 0, \tag{28}$$

these conditions are intuitive as one would expect the Planck mass and the sound speed to be real properties. A modified density perturbation equation can now be formulated from the modified Poisson equation. Furthermore, by changing the time derivatives of Eq. 22 to ones with respect to $\ln a$, the modified density perturbation equation of the EFT is given as,

$$\delta'' + \left(2 + \frac{H'}{H}\right)\delta' = \frac{4\pi G_N \rho_m}{H^2}\mu\delta. \tag{29}$$

Finally, we now have a theory which describes matter and potential perturbations with a new vacuum energy scalar field that couples to the metric. The perturbation equations contains only four free functions: M^2, α_K, α_B and H, where H relates to Ω, Λ, Γ through the modified Friedmann equations [18].

4 Numerical Methods

Now equipped with a relatively simple stable general theory of UG, a vast horizon of new physics can be explored. Adhering to this, it would be worthwhile to determine some recognisable properties. The abstract nature of the α parameters would undermine any contrasting predictions UG has relative to ΛCDM. Therefore, to obtain an intuitive understanding of the predictions of UG, it is constructive to describe it in terms of M^2 and c_s^2. This may provide a rudimentary insight into the equation of state of dark energy and its relationship with the metric.

This section outlines the methods used to obtain the present day values of the Planck mass and sound speed as described by the EFT of modified gravity. Firstly, the theory was reparameterised to fully described by these two parameters. Secondly, the perturbation equations were numerically integrated to obtain the evolution of δ, Ψ and Φ under some given present Planck mass and sound speed values. Finally, the LSS growth rate, $f\sigma_8(a)$, and *Planck* CMB power spectrum data were compared to theoretical UG predictions with a multivariate χ^2 fit to constrain M_0^2 and $c_{s,0}^2$.

4.1 Constraining Horndeski Gravity

4.1.1 Background

Despite the search beyond concordance cosmology, ΛCDM accurately describes the evolution of the universe. Therefore, it is reasonable to adopt its description of the background. This greatly simplifies the framework and allows any deviations from the model to be immediately discernible. Therefore, Friedman dynamics can be applied,

$$H^2 = H_0^2 \left(\Omega_m a^{-3} + \Omega_\Lambda\right), \tag{30}$$

where the universe is assumed to be matter dominate at recombination with no radiative contribution. Moreover, the observational values of $\Omega_m = 0.315$ and $\Omega_v = 1 - \Omega_m = 0.685$ (assuming a flat universe) are applied here and throughout from *Planck* [21].

4.1.2 Perturbations

With the background cosmology being described by ΛCDM, only the perturbation equations are altered. In the interest of identifying the modified values of M^2 and c_s^2, it is necessary to redefine the§ UG perturbation equations solely in terms of these parameters. Unfortunately, this isn't entirely possible as α and α_B can't be simultaneously described by c_s^2. For this reason a degenerate parameter of $\xi \equiv \alpha c_s^2$ is used and the set of free EFT functions $\mathcal{H} = \{M^2, \xi\}$ are hereby defined. By making the substitution $B = (1 + \alpha_B)$, Eq. 27 can be rearranged,

$$B' + B^2 - B\left(1 + \alpha_M + \frac{3}{2}\Omega_m(a)\right) + \frac{1}{2}\left(\xi + 3\Omega_m(a)\right) = 0, \tag{31}$$

where $H'/H = -\frac{3}{2}\Omega_m(a)$ (see Ap. A.1.1) and $\rho_m/2H^2M^2 = \frac{3}{2}\Omega_m(a)$ (see Ap. A.1.2), where $\Omega_m(a) \equiv \Omega_m a^{-3}/(\Omega_m a^{-3} + \Omega_v)$. Consequently, α_B and the modification parameters μ and γ can now be fully specified by $\mathcal{H}$ alone.

4.2 Modified Cosmological Perturbations

To study the predictions of UG, $\xi(a)$ and $M^2(a)$ must first be specified. Of course given their contrived nature, one is free to choose any formalism. However, there are logical constraints that can be imposed. Given that the scalar field, ϕ, represents a dynamical vacuum energy, it's expected that it would have only become significant 4 billion years ago and can be traced by $\Omega_\Lambda(a) \equiv \Omega_\Lambda/(\Omega_m a^{-3} + \Omega_\Lambda)$. Subsequently, it can be argued that $\mathcal{H}$ will only deviate from their ΛCDM values, $\mathcal{H}_{\Lambda\text{CDM}} = \{1, 0\}$, when the vacuum energy becomes significant,

$$\mathcal{H}(a) = \mathcal{H}_{\Lambda\text{CDM}} + (\mathcal{H}_0 - \mathcal{H}_{\Lambda\text{CDM}})\,\frac{\Omega_\Lambda(a)}{\Omega_\Lambda} \tag{32}$$

where $\mathcal{H}_0$ are the present-day values of each parameter. Notice that $\alpha_M = 3\Omega_m(a)(1 - 1/M^2)$ from this formalism. With a full description of the modification parameters, the perturbations can be determined. As with Eq. 31, similar substitutions can be applied to the modified potential (Eq. 23) and density (Eq. 29) perturbation equations,

$$\nabla^2\Psi = -\frac{3}{2}H_0^2\Omega_m\mu a^{-1}\delta, \tag{33}$$

$$\delta'' + \left(2 - \frac{3}{2}\Omega_m(a)\right)\delta' = \frac{3}{2}\Omega_m(a)\mu\delta. \tag{34}$$

Naturally, it is simpler to work in Fourier space for Poisson's equation, $\nabla^2 \to k^2$,

$$\Psi_k = -\frac{3}{2}H_0^2\Omega_m\mu(a)a^{-1}\delta_k/k^2. \tag{35}$$

Furthermore, $\langle|\delta_k|^2\rangle \propto k^3P(k)$. Where $P(k)$ is the matter power spectrum which $\propto k^{n_s}$ at large scales where $n_s = 0.965 \approx 1$ [21] is the scalar spectral index. This removes the scale dependence of Ψ_k, however, it is must to be normalised to the CMB,

$$\Psi_k = -\frac{3}{2}H_0^2\Omega_m\mu(a)a^{-1}\delta_k/\delta_{k,\text{CMB}}\left(\frac{A_s}{k_0^2}\right)^{1/2}. \tag{36}$$

Where $\delta_{k,\mathrm{CMB}}$ is the calculated matter perturbation at the CMB, $A_s = 2.101 \times 10^9$ is the primordial comoving curvature power spectrum amplitude which is defined at $k_0 = 0.05$ Mpc [21].

To solve the matter perturbation equation numerically, it was discretised. Using $y \equiv \delta'$ and $y' = (y_{i+1} - y_i)/\Delta \ln a$, the i^{th} step of Eq. 34 can be written as,

$$y_{i+1} = y_i + \left(\frac{3}{2}\Omega_m(a)\mu\delta - \left(2 - \frac{3}{2}\Omega_m(a)\right) y_i\right) \Delta \ln a. \tag{37}$$

Here, $\Delta \ln a \ll 1$ is an integration 'time-step'. With initial values δ_0 and y_0 the differential equation can be solved over a series of time-steps for y. Similarly, $\delta_{i+1} = \delta_i + y_i \Delta \ln a$ was calculated at each step to calculate the evolution of δ. A similar method was applied to the Eq. 31 to obtain a discrete description of α_B. Subsequently, a `python` program was constructed to numerically solve these equations. Finally, the gravitational potentials were calculated using Eq. 36.

4.3 Comparison with Data

4.3.1 Cosmic Microwave Background

The CMB is observed as a plane of radiation on the sky and therefore its temperature fluctuations require a 2D treatment. However, as the sky isn't truly flat, perturbations are expanded in spherical harmonics, Y, with scales being labelled by multipole number, ℓ,

$$\Theta(\vec{n}) \equiv \frac{\delta T}{T}(\vec{n}) = \sum_{\ell=0}^{\ell=\infty} \sum_{m=-\ell}^{m=\ell} a_{\ell m} Y_{\ell m}(\vec{n}), \tag{38}$$

where $a_{\ell m} = \int_{-\pi}^{\pi} \int_0^{2\pi} \Theta Y^*_{\ell m} d\Omega$ and Ω is the solid angle projected on the sky. From orthonormality of the harmonics, the variance of temperature fluctuations is given as,

$$\langle \Theta^2 \rangle = \frac{1}{4\pi} \sum_{\ell,m} |a_{\ell m}|^2 = \frac{1}{4\pi} \sum_{\ell} (2\ell + 1) C_\ell, \tag{39}$$

where there are $2\ell + 1$ modes per ℓ and C_ℓ is the angular power spectrum. Thus, sources of temperature fluctuations of the CMB can be identified in its measured power spectrum. There are multiple sources of temperature fluctuations that can be split into two main categories: primary and secondary anisotropies. Primary anisotropies occur at the time of last scattering. As the universe becomes transparent at recombination, photons are free to travel in a straight line. If a photon is within an overdense region at this time, it will become redshifted as it climbs out of the potential-well. Consequently, there is a direct link between

this change in wavelength (or temperature) with the change in gravitational potential from the background, $\Theta \sim \Psi$. However, due to time dilation that occurs at last scattering, the universe appears younger and hotter. In the early universe $a \propto t^{2/3}$ (matter dominated) and $T \propto a^{-1}$ meaning that $\Theta \sim -(2/3)\Psi$. Thus, this gives a total contribution of,

$$\Theta_{\rm SW} = \frac{1}{3}\Psi. \tag{40}$$

This is known as the Sachs-Wolfe effect (SW) (see Ref. [52]) and is the main source of primary anisotropies. There are other effects, such as non-zero velocity plasma at recombination. This results in Doppler shifted radiation and hence temperature fluctuations. However, these perturbations are damped out by cosmic expansion and occur on much smaller scales.

Furthermore, second anisotropies occur along the line of sight and are usually a consequence of interactions with matter. As radiation travels through space it may enter overdense regions and subsequently fall into their potential-wells resulting in blueshift. In a matter dominated universe, the radiation will be subject to the same degree of redshift as it leaves the well and the effect neutralises. However, in a vacuum dominated universe, photons travel through overdensities that evolve to a less dense state under cosmic acceleration. This leaves a net effect and results in temperature fluctuations of photons and the CMB. This is called the Integrated Sachs-Wolfe effect (ISW) and can be described as,

$$\Theta_{\rm ISW} = \int_{-3}^{0} d\ln a \left(\Phi' + \Psi'\right). \tag{41}$$

Here the integral limits represent the scale factor at recombination and present-day in log-space, respectively. It is possible to probe UG through its potentials' evolution and comparing their resulting temperature fluctuations with the CMB power spectrum. As previously discussed, the regime of UG is of large scales where only gravity and the vacuum are of significance; these scales correspond to small ℓ. Fig. 1 shows the power spectrum of the CMB from *Planck*. The initial tale of the spectrum, $\ell \leq 30$, is dominated by ISW. Therefore, this *Planck* data was used to compare with the theory. The ΛCDM model predicts lower temperature fluctuations than observed. However, the free functions of $\mathcal{H}$ allow UG's potentials to be modified such that the temperature fluctuations fit to observations. *Planck* predicts that within MG and DE models that $\mu_0 > 1$ and $\gamma_0 > 1$ [21]. Therefore, a naïve prediction would be that the strength of gravity needs to be reduced ($M^2 < 1$) to enhance the ISW and raise temperature fluctuations. The CMB power spectrum is scale-dependent whereas $\mathcal{H}$ are not. Nevertheless, Θ is relatively constant with ℓ at low values. This removes a need for scale dependence and UG predictions can be treated as a straight line in this regime.

To calculate the derivatives of the potentials and subsequently, the ISW, the `python` package `scipy` was implemented. Subsequently, the total CMB temperature fluctuations could be calculated,

$$\Theta^2_{\rm CMB} = \Theta^2_{\rm SW} + \Theta^2_{\rm ISW}. \tag{42}$$

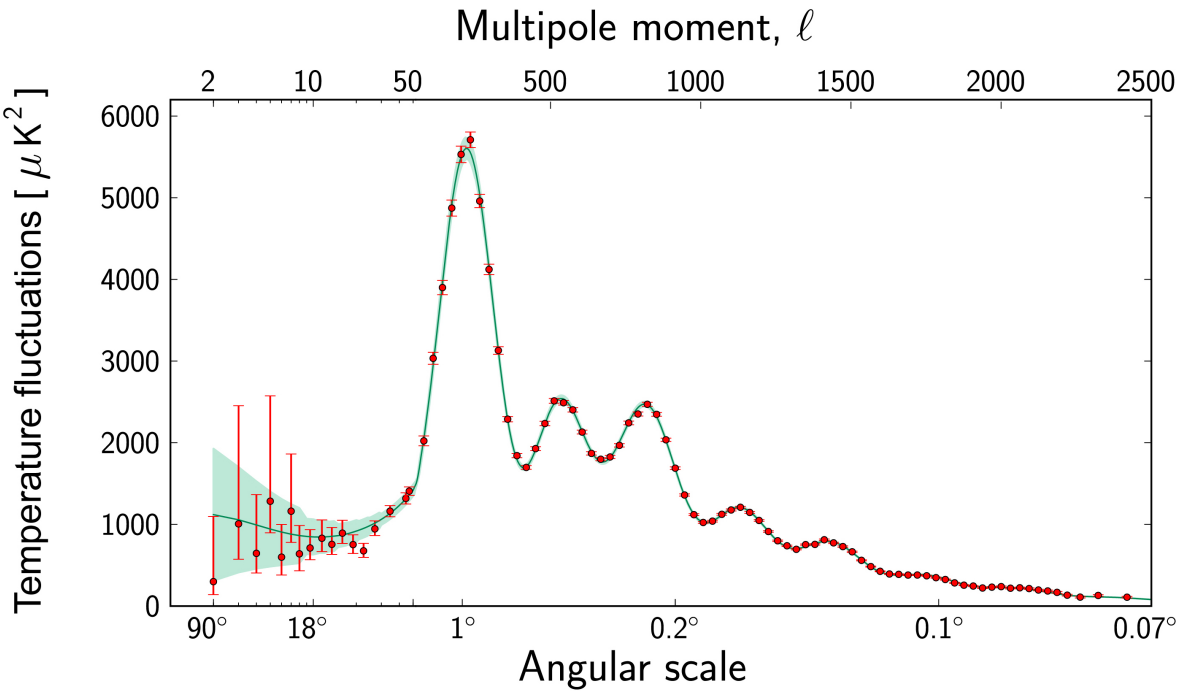

Figure 1. The CMB power spectrum as seen by *Planck* [21]. There is a large degree of uncertainty where $\ell \leq 30$. This is marked by the error bars on the data points and the shaded green area. This is the regime that UG is compared to. The theoretical ΛCDM line is sits slightly below the data points. Intuitively, it was expected that a decrease in M^2 would fit to the data.

From here a series of χ^2 tests were computed over a given parameter space to fit to the data,

$$\chi^2 = \sum_i \left(\frac{\Theta_i - \Theta_{\rm CMB}}{\sigma_i} \right)^2 . \tag{43}$$

Where Θ_i and σ_i are the *Planck* data points and uncertainties, respectively, and $\Theta_{\rm EFT}$ is the constant EFT prediction. Furthermore, the 68.3% and 95% confidence levels of the these tests were calculated. This was achieved by determining where $\chi^2 = \chi^2_{\rm min} + \Delta\chi^2$ for $\Delta\chi^2 = 2.3, 5.99$, respectively.

4.3.2 Large Scale Structure

As well as the potentials, matter perturbations of UG were investigated by comparing its evolution to observational data. This can be achieved by considering the LSS growth rate, $\Pi(a) \equiv f(a)\sigma_8(a)$. Here $f(a) \equiv d\ln\delta/d\ln a$ is the growth rate of linear matter perturbations and $\sigma_8(a)$ is the matter power spectrum on scales of $8h^{-1}$ Mpc where $h \equiv H_0/(100$ km s^{-1} Mpc$^{-1})$. Using the definition $\sigma_8(a) = \frac{\sigma_8}{\delta(1)}\delta(a)$, the structure growth rate can be expressed as,

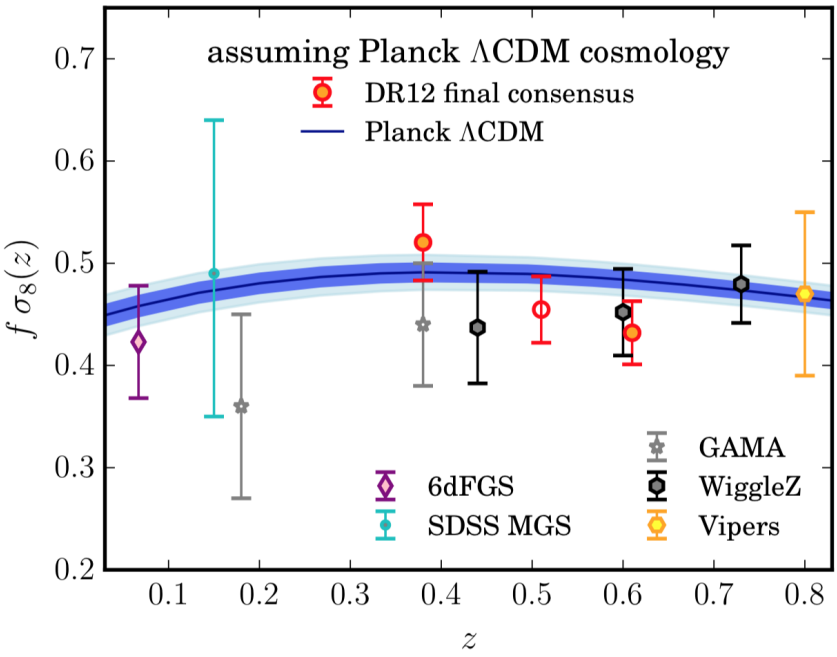

Figure 2. $\Pi(z) \equiv f\sigma_8(z)$ observational data compared with ΛCDM as seen in Ref. [53]. The model line appears to sit slightly above the data. It was expected that an increase in M^2 would lower the theoretical line and fit with the data.

$$\Pi(a) = \frac{\sigma_8}{\delta(1)}\delta'(a), \tag{44}$$

where $\sigma_8 \equiv \sigma_8(1) = 0.811$ [21] and $\delta(1)$ is the present-day matter perturbation used to normalise Π. This is easily calculated from the matter perturbations and was compared to data. Observable data was taken in a range of 0.34–1 of a from a wide range of papers [53–81]. A compilation of the full data set and their surveys can be found in Ref. [82]. Again, a similar χ^2 test was applied to UG and the data to identify the best fit parameters of $\mathcal{H}_0$. Fig. 2 shows a sample of the observational data with $z = a^{-1} - 1$. There is a steady linear increase of growth at high z when the universe is matter dominated. At low z the universe becomes vacuum dominated and results in a suppression of growth as conveyed by the downward curve of Π. Evidently, the ΛCDM prediction appears slightly to high compared to the observational data at low z. In this case, it is clear that $\mu_0 < 1$ is requires to fit to the data. Consequently, an intuitive prediction would be that the strength of gravity must be decreased ($M^2 > 0$) to lower the downward curve.

This prediction conflict with the CMB prediction. Nevertheless, these are only conjectures of UG under the parameterisation used in this project. What can be stated is that the growth of matter requires additional suppression as the universe becomes vacuum dominated — $\mu < 1$ at late times, and an increase of μ and γ of some form to raise CMB fluctuations. Furthermore, it should be stated that the ΛCDM model predictions are not inconsistent with the data. However, it is constructive to investigate where the model appears slightly amiss and to identify if these independent observations produce consistent alternative results.

5 Results & Analysis

5.1 Effective Field Theory

As shown above, UG contains complex cumbersome differential equations with various free parameters. Initially, in order to explore the theory limits, the modified cosmological perturbations were specified by α_B as well as $\mathcal{H}$. A similar parameterisation to Eq. 32 was applied, $\alpha_B = \alpha_{B,0}\Omega_\Lambda(a)$. This limited numerical integration and allowed the base theory to be tested. Despite this, the degeneracy of ξ and the abstract nature of α_B posed challenges to identify the theorem's bounds of stability.

Naturally, this began with a reproduction of density perturbations in Einstein-de Sitter (EdS) — $\Omega_m(a) = 1$ and $\Omega_\Lambda(a) = 0$, and ΛCDM cosmology. In both cases $\mu(a) = 1$ ($\mathcal{H} = \{1, 0\}$) with $\delta \propto a$ with the exception of ΛCDM exhibiting a suppression of growth as the vacuum becomes significant. Immediately, this caused a divergence of μ in Eq. 25 as $\xi = 0$. This is easily solvable for ΛCDM as $\mu = 1$ at all times. However when $M^2 \neq 1$, α_B and therefore α deviate from zero. Therefore, it must be asserted that $c_s^2 \neq 0$ to prevent instability of the parameterisation of μ. Consequently, the case where the vacuum energy acts like pressureless dark matter ($c_s^2 = 0$) is excluded from the theory. Nevertheless, numerical issues continued to ensue when $\xi \ll 1$ causing μ to diverge. However, this was mainly due to the contrived parameterisation of α_B which suppresses μ when specified by ξ and α_M. This wasn't anticipated and consequently, remained an unsolved problem until Eq. 31 was implemented to determine α_B in terms of $\mathcal{H}$. Once this was introduced, δ became well defined and behaved as expected. Fig. 3 shows the density perturbation evolution in E-dS, ΛCDM and UG with $\mathcal{H}_0 = \{1.2, 0.2\}$. This corresponds to an initial increase of μ when $\xi \ll 1$. At this time the universe is matter dominated which results in a high growth rate. Subsequently, when the vacuum energy starts to dominate, the $\mathcal{H}$ parameters increases quickly resulting in a sharp decrease in μ. Nevertheless, the large increase in growth rate at early times results in greater density perturbations than ΛCDM.

Furthermore, it is interesting to identify the behaviour of the matter density perturbations over a range of present-day values $\mathcal{H}_0$. It's expected that these parameters will produce density perturbations on the same order as ΛCDM. This corresponds to values of $\mathcal{O}(M^2) \sim 1$ and $\mathcal{O}(|\alpha_i|) \lesssim 1$ for all i. With $0 < c_s^2 \leq 1$, it was expected that ξ must have similar limits. Figure 4 illustrates how the density perturbations diverge from ΛCDM by varying M_0^2 and ξ_0 independently. Intuitively, there are higher density perturbations when $M_0^2 < 1$ as this corresponds to an enhancement of the strength of gravity. Moreover, as M_0^2 increases and approaches 1, the perturbations decrease accordingly. However, as the Planck mass increases above 1, the perturbations exhibit a turnaround and enhance. Again, this is a consequence of an initial increase in μ before the vacuum becomes significant. Once the vacuum is dominant and μ decreases, there is a turnoff of growth and even a reverse of growth where $M_0^2 = 1.3$. The increasing values of early-time μ with M^2 can be attributed to its growth rate, α_M and small ξ.

It is more challenging to interpret the change in ξ_0 as it contains α. Here $M_0^2 = 0.8$ in each case. An increase in ξ_0 corresponds to a suppression of growth; this is always true when

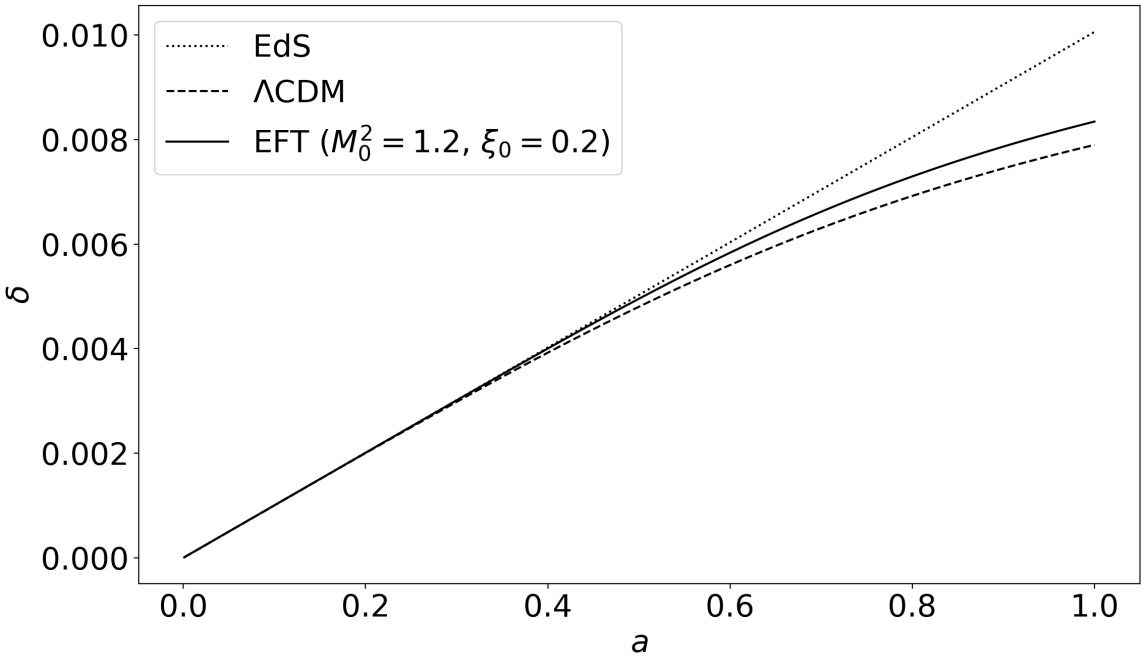

Figure 3. Matter density perturbations in different cosmological regimes. Linear growth occurs in EdS cosmology as shown by the dotted line. ΛCDM (dashed line) exhibits a decline in growth due to the cosmological constant. UG exhibits an enhancement of growth despite the decrease of the strength of gravity at late times ($M^2 > 1$). This can be explained by the early-time increase in μ due to $M^2 \neq 1$ and the small value of ξ_0.

$M^2 \neq 1$ and $\alpha_M \neq 0$. However when $M^2 = 1$, ξ enhances the perturbations. This illustrates that M^2 has a notable enhancing effect on μ at early times via α_M. Qualitatively, when ϕ couples to the metric, its effect on gravity at early times is great enough to overturn the effect of ξ. Despite the attempt to define UG in terms of the intuitive parameters $\mathcal{H}$, the intricate parametrisation of μ produces abstruse predictions.

The potentials exhibited similar behaviour to the matter perturbations. The temporal potential, Ψ, mirrored μ with an initial increase when ξ is small and subsequently adhered to its expected decay or enhancement accordingly with M_0^2. It is clear from the evolution of Ψ, that the present-day location of the gravitational field is dominated by M^2. Moreover, ξ determines the path of evolution of Ψ with more extreme paths occurring as ξ_0 decreases. The spatial potential, Φ, is calculated from the anisotropic stress γ. This has an interesting effect where the evolution of Φ is consistent with Ψ except the initial increase is removed. This is because γ exhibits a similar evolution to μ but with an early-time decrease. Figure 5 illustrates the evolution of the potentials where $M_0^2 = 1.2$ is set constant and ξ_0 varies. The potentials decay below ΛCDM in concordance with the enhanced strength of gravity. An increase of ξ_0 slightly suppresses this decay as well as the initial enhancement of Ψ. Similarly, if M_0^2 varies with a constant ξ_0, the potentials enhance as M_0^2 decreases (see Ap. B.1). Again, γ removes initial growth in Φ and seemingly simplifies its evolution.

The predictions of UG are predominantly intuitive under the parameters, $\mathcal{H}$. An increase in M_0^2 decreases the gravitational potentials at late times accordingly. Additionally, ξ_0 appears

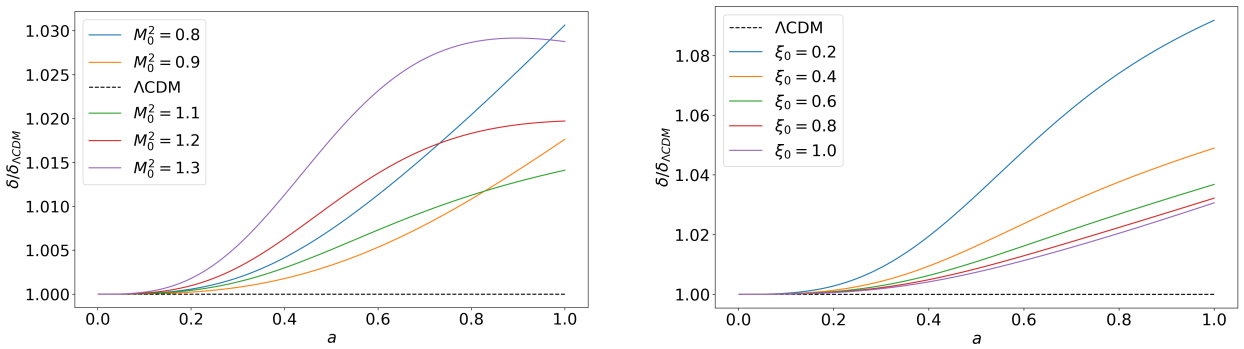

Figure 4. Left: Matter perturbations of UG compared to ΛCDM with varying M_0^2 and constant $\xi_0 = 0.6$. Perturbations are enhanced when $M^2 \neq 1$ through α_M and low ξ_0 at early times. Subsequently, there is a cut-off of growth as the vacuum dominates when $M_0^2 > 1$ and an increase when $M_0^2 < 1$. Right: Similar plot but with fixed $M_0^2 = 0.8$ and varying ξ_0. With a higher strength of gravity there is a general increase of the perturbations. There is a suppression of growth as ξ_0 increases as early-time μ decreases. Additionally, larger values of ξ_0 enhance growth at late times as shown by the perturbation tails. Notice the blue line of the left plot and green of the right correspond to the same cosmology.

to enhance the present-day potentials as it increases. However, the parameterisation of μ allows an enhanced growth rate when the universe is matter dominated and ξ is small. Thus, smaller values of ξ_0 correspond to higher growth rates at early times. Conversely, anisotropic stress removes the early time enhancement of Ψ and produces a clear correlation between ξ and Φ. The density perturbations cumulatively convey these properties. When ξ_0 is small, there is an increased growth rate at early times which is sufficiently high that it dominates over the subsequent suppression as the vacuum becomes significant. This is conveyed in Fig. 5. This is also the case for M^2 as it deviates from 1. Regardless of whether the M^2 increases or decreases, $\alpha_B - \alpha_M$ enhances μ at early times resulting in higher cumulative growth. Again, once the vacuum is significant, the appropriate behaviour of the density perturbations occur with respect to M^2.

5.2 Fitting to the CMB

The potentials and their evolution were then used to calculate the SW and ISW to obtain temperature fluctuations in the CMB. This produced a scale-invariant straight line that is sufficient for $\ell \leq 30$. Again, it was worthwhile to ensure that ΛCDM predictions could be reproduced. This was successful with the theoretical ΛCDM line sitting under the observational data. This can be seen in Fig. 6 which shows a line of best fit using a χ^2 test. A range of $\mathcal{H}_0$ values satisfied this fit. The complex parameterisation of μ and γ allow various $\mathcal{H}_0$ values that produce similar ISW effects. Moreover, the sensitivity and effect of each parameter are dependent on one another. Therefore, describing the effect that M^2 and ξ have on the ISW, is non-trivial. Subsequently, a series of χ^2 tests were carried out over a range of values of $\mathcal{H}_0$. As anticipated, this produced a degenerate line of best-fit values as two parameters are determining a single degree of freedom. Furthermore, due to the complex parameterisation of μ, this degenerate line exhibits a curve. Figure 7 is a χ^2 contour

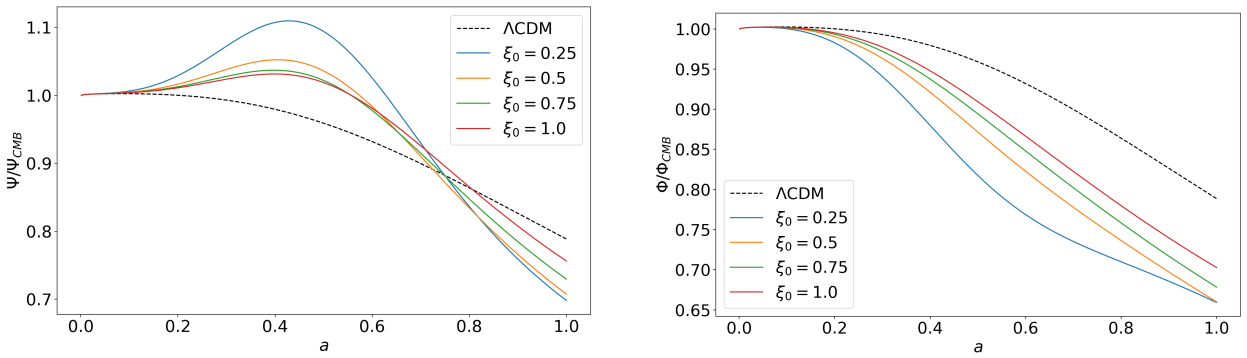

Figure 5. Left: Evolution of Ψ with varying ξ_0 at constant $M^2 = 1.2$. Lower value of ξ_0 enhance μ and subsequently, Ψ at early times. The late-time decrease can be attributed to M^2. Lower values of ξ_0 reduced Ψ further at late times and accounts for the tail of the density perturbations in Fig. 4. Right: Evolution of Φ in the same regime. This comparable to the evolution of Ψ except the early enhancement of the potential is absent. This due to the formalism of γ which is small at early times in this regime.

plot which displays this degenerate line. Immediately, it can be seen that UG favours an enhanced M_0^2. This suggests that ϕ couples to the metric and reduces the strength of gravity as the universe becomes vacuum dominated.

This is an interesting result as it was expected that to increase $\Theta_{\rm CMB}$, the strength of gravity must also increase (reduced M_0^2). However, as previously discussed, the early-time increase of μ is proportional to M_0^2 through α_M. This subsequently perturbs Ψ and results in a higher ISW effect. Figure 7 shows that $\Theta_{\rm ISW}$ is insensitive to ξ_0 when $M^2 \sim 1.25$. The upwards curve of the degenerate line is more difficult to interpret physically. However, there is an inclination to discard this prediction as a feature of the model. This is argued under the assumption that $M_0^2 \sim 1$ and is close to the ΛCDM value. This is supported by the LSS prediction (see Sec. 5.3).

Across the horizontal degenerate line, UG predicts a value of $\mu_0 \sim 0.85$ and $\gamma_0 \sim 0.93$ in contrast with the *Planck* CMB value of 1.1 and 0.22 [21], respectively. However, this paper assumes a parametrisation of μ and γ similar to Eq. 32. This only allows the parameters to travel in a single direction. Despite UG predicting a reduced value of μ_0, due to early-time enhanced growth, it is clear that it is the parametrisation of μ and γ of *Planck* that is at odds with UG rather than their present-day values.

5.3 Fitting to the LSS

The LSS growth rate proved to be less degenerate as it only specific $\mathcal{H}_0$ values exhibit a late-time reduction of Π from ΛCDM. Again, this can be explained by the parameterisation's inherent early-time enhancement of μ. Any deviation of M^2 from 1 results in an early-time enhancement of δ and therefore Π. However, the expected late-time suppression of Π with increasing M_0^2 was present. This behaviour is a reflection of the density perturbations as

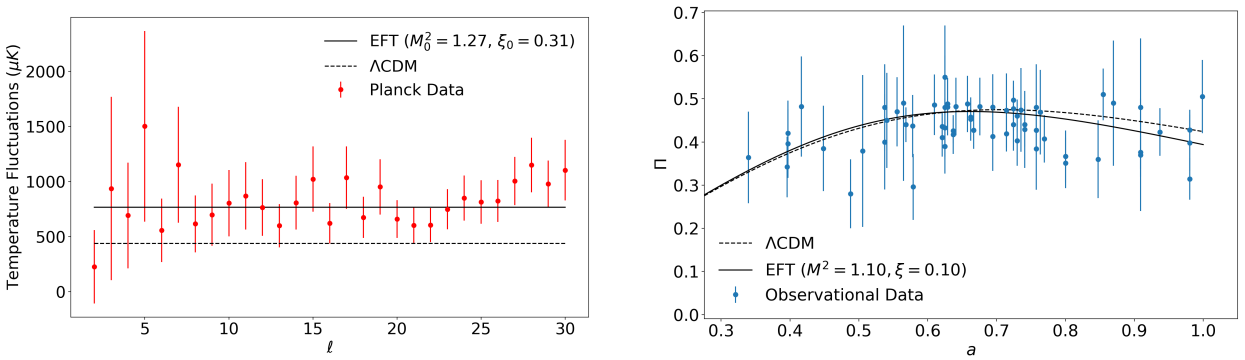

Figure 6. Left: Large scale observational temperature fluctuations of the CMB power spectrum as seen from *Planck* [21] (red data points). The dashed line conveys the scale invariant ΛCDM prediction which sits below the data. The solid line represents the prediction of UG with an example of the best fit parameters, $M^2 = 1.27$ and $\xi_0 = 0.31$. Right: The blue data points are observational data of $\Pi(a)$ from a wide range of surveys [53–81]. Again the dashed line represents the ΛCDM prediction and the solid represents the best fit of UG with $M^2 = 1.1$ and $\xi_0 = 0.1$.

discussed above. Consequently, the early-time enhancement and late-time suppression of Π both increase with M^2. This only permits a narrow margin of M_0^2 values that result in a late-time reduction of Π in relation to ΛCDM. Additionally, ξ competes with M^2 by increasing late-time Π. Consequently, the model favours a small ξ_0 despite this resulting in a larger early-time enhancement of growth.

Fig. 6 shows the LSS growth rate of the best-fit values of $\mathcal{H}_0$. These parameters allow for the greatest late-time suppression within the parameter space. This raises a concern of a possible inherent issue with the parameterisation of the EFT. Nevertheless, the best-fit parameters are fairly consistent with the CMB as shown in Fig. 7. Furthermore, the LSS fit predicts $\mu_0 \sim 0.93$ which is consistent with the reduced value from the CMB. The parameterisation of the EFT solves the conflicting predictions of μ_0 from the CMB and LSS.

Fig. 7 shows the best-fit parameters of $\mathcal{H}_0$ using a χ^2 fit for the CMB (red contour), LSS (blue contour) and a combination of the two (grey contour),

$$\chi^2_{\rm UG} = \chi^2_{\rm CMB} + \chi^2_{\rm LSS}. \tag{45}$$

The dark and light contours represent the 68% and 95% confidence levels, respectively. From both fits, UG is consistent in predicting an enhanced present-day Planck mass value. Despite this, there is no clear prediction for ξ_0. As illustrated in Fig. 6, the LSS observational data contains a larger degree of scatter. This meant that $\chi^2_{\rm CMB}$ dominated and shifts the collective $\chi^2_{\rm UG}$ to its results. The collective fit predicts that $\xi_0 \geq 0.26$ and $1.11 \leq M_0^2 \leq 1.28$ at a 95% confidence level in the given parameter space. This corresponds to a reduction in gravitational strength as ϕ becomes significant. Again, the intricate parameterisation of μ allows this to be a consistent prediction for seemingly conflicting observations.

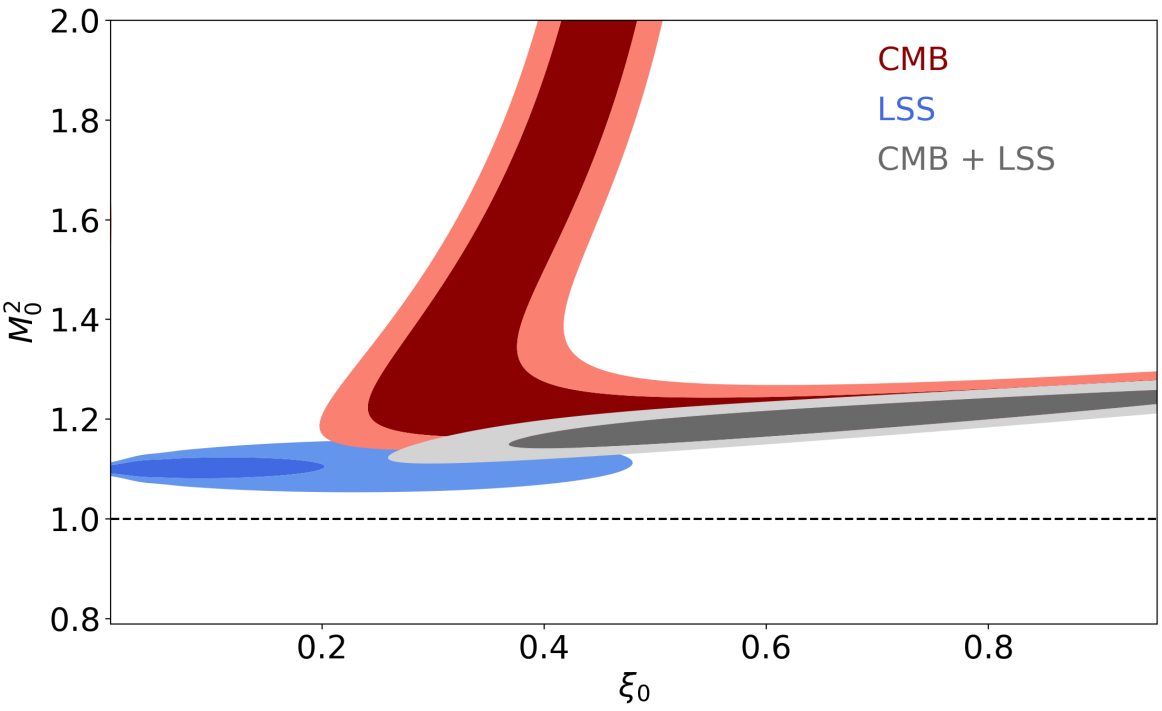

Figure 7. Parameter constraints of M_0^2 and ξ_0 from χ^2 fits. The dark and light contours represent the 68% and 95% confidence levels, respectively. The fit to the CMB power spectrum (red) and the fit to the LSS growth rate (blue) show a fairly consistent result of an enhanced M^2 but both display a large degeneracy of ξ. The grey contour conveys a combined fit constraining $1.11 \leq M_0^2 \leq 1.28$. The CMB fit dominates over the LSS as this is a better fit (see Fig 6) and shifts the grey contour.

6 Future Application

The EFT of UG has predicted some interesting results that may offer an alternative description of the cosmos. However, the simplified formalism adopted in this project only offers an inkling of this new realm of cosmology. Concerning this project, further analysis could be applied to the formalism. Firstly, a covariance test of M_0^2 and ξ_0 could be applied to reveal any correlation between the parameters. This would reveal whether the parametrisation used in this project is suitable to obtain UG's predictions. Additionally, it may have been constructive to expand the parameter space into $\xi_0 > 1$; especially as this parameter is more difficult to predict. Nevertheless, if near ΛCDM solutions are assumed, this parameter range is arguably sufficient. Furthermore, it would be useful to examine the μ and γ parameters in more detail. The inherent early-time increase allows μ to evolve either side of 1 resulting in a more exotic history of LSS growth. Like with the LSS and the CMB, there are multiple alternative observational probes which could allow UG to be constrained further. This includes weak gravitational lensing, baryon acoustic oscillations and supernovae. This would allow for independent best-fit parameter tests that may break the degeneracy of the results found here.

This project attempted to stay as general as possible in its theoretical approach. However,

some generality was ceded for simplicity. Firstly, the project aimed to describe UG with just two free parameters. The more rigorous approach would be to describe the theory in terms of all its free parameters: c_s^2, M^2 and all of the α parameters. However, this would require substantially more time to investigate. Furthermore, the background cosmology was described by ΛCDM. Again, this could be described by the full extent of UG but this would drastically increase the number of free parameters. However, a future investigation could allow a dynamical w to allow a more general background. Tight constraints on this parameter already exist which could break the degeneracy of the sound speed.

In the advent of deep space surveys such as *Euclid* [83], it is of great interest to cosmology that a stable and general EFT of UG is available. This survey aims to significantly constrain dark energy parameters. In turn, this will narrow the vast scope of MG and dynamical vacuum energy models. Further progression and investigation into the parameterisation of UG is imperative to accurately interpret the coming observational data.

7 Conclusion

The late-time acceleration of the universe was one of the most pivotal discoveries in modern physics. This realisation thrust the ΛCDM model to the forefront of cosmology and has endured two decades of scrutinous examination. This model has accounted for the vast wealth of independent observational probes such as the CMB and LSS. The main feature of this model is the cosmological constant, Λ, which is a natural product of Einstein's general relativity. This fundamental property of the vacuum is believed to account for $\sim 70\%$ of the mass-energy budget of the universe and is responsible for its acceleration. However, quantum field theory predictions and observational values for the vacuum energy are a colossal 10^{60} orders of magnitude out. Consequently, ΛCDM requires an exceedingly high degree of fine-tuning and calls the model into question.

Subsequently, the past two decades has brought forth an abundance of alternative dark energy and modified gravity models acquit of fine-tuning. However, it is important to develop general unified frameworks that enable efficient predictions for current and future observations. The effective field theory of dark energy and modified gravity aims to achieve this goal. UG is embedded on Horndeski gravity which ensures that it remains as general and stable as possible. The free parameters of the theory allow the fitting of theory to observations rather than the opposite. The main feature of this theory is that it replaces the cosmological constant, Λ, with a dynamical vacuum energy scalar field which couples to the metric, $\phi(a)$. However, the formalism of this theory is still under development and currently contains a variety of indiscernible free parameters.

This project investigated this EFT of UG and attempted to reduce its free parameters through specification or degeneracy. More specifically, to describe matter density perturbations and gravitational potentials in terms of the intuitive parameters, the Planck mass, M, and the sound speed of ϕ, c_s. However, these two parameters cannot fully describe UG alone, and so the degenerate parameter $\xi \equiv \alpha c_s^2$ was used instead. These parameters were then

fit to the CMB angular power spectrum and LSS growth rate to determine the present-day values, M_0^2 and ξ_0. Naïve predictions of $M_0^2 > 1$ and $M_0^2 < 1$ for the LSS and CMB were expected, respectively. However, the complex parameterisation of μ contained an unanticipated feature of early-time growth enhancement. This produced consistent results of $M_0^2 > 1$ for each observation. A combined χ^2 fit to the CMB and LSS provided results of $\xi_0 \geq 0.26$ and $1.11 \leq M_0^2 \leq 1.28$ at a 95% confidence level (in the parameter range $0 \leq \xi_0 \leq 1$).

This result is a success for UG and illustrates that the seemingly opposing observations can be accounted for under this parameterisation. With more stringent constraints on dark energy and cosmological parameters on the horizon, it is imperative that we meet these observations with an alternative generalised theory to better describe the universe around us.

References

[1] Adam G. Riess et al. Observational Evidence from Supernovae for an Accelerating Universe and a Cosmological Constant. *The Astronomical Journal*, 116(3):1009–1038, Sep 1998.

[2] S Perlmutter et al. Measurements of Ω and Λ from 42 High-Redshift Supernovae. *The Astrophysical journal.*, 517(2):565–586, 1999.

[3] Joshua A. Frieman et al. Dark Energy and the Accelerating Universe. *Annual Review of Astronomy and Astrophysics*, 46(1):385–432, 2008.

[4] Ronald J. Adler et al. Vacuum catastrophe: An elementary exposition of the cosmological constant problem. *American Journal of Physics*, 63(7):620–626, 1995.

[5] Timothy Clifton et al. Modified Gravity and Cosmology. *Physics Reports*, 513(1-3):1–189, Mar 2012.

[6] Clifford M. Will. The Confrontation between General Relativity and Experiment. *Living Reviews in Relativity*, 17(1):4, Jun 2014.

[7] Edmund J. Copeland, M. Sami, and Shinji Tsujikawa. Dynamics of dark energy. *International Journal of Modern Physics D*, 15, May 2012.

[8] Jaewon Yoo and Yuki Watanabe. Theoretical Models of Dark Energy. *International Journal of Modern Physics D*, 21(12), Nov 2012.

[9] Jolyon K Bloomfield and Éanna É Flanagan. A Class of Effective Field Theory Models of Cosmic Acceleration. *Journal of Cosmology and Astroparticle Physics*, 2012(10), Oct 2012.

[10] Raul Jimenez, P. Talavera, and Licia Verde. An effective theory of accelerated expansion. *International Journal of Modern Physics A*, 27(30), Dec 2012.

[11] Giulia Gubitosi et al. The Effective Field Theory of Dark Energy. *Journal of Cosmology and Astroparticle Physics*, 2013(02), Feb 2013.

[12] Eric V. Linder et al. Is the Effective Field Theory of Dark Energy Effective? *Journal of Cosmology and Astroparticle Physics*, 2016(05), May 2016.

[13] Antonio De Felice et al. On the stability conditions for theories of modified gravity in the presence of matter fields. *Journal of Cosmology and Astroparticle Physics*, 2017(03), Mar 2017.

[14] Joe Kennedy, Lucas Lombriser, and Andy Taylor. Reconstructing Horndeski theories from phenomenological modified gravity and dark energy models on cosmological scales. *Physical Review D*, 98(4), Aug 2018.

[15] Gregory Walter Horndeski. Second-Order Scalar-Tensor Field Equations in a Four-Dimensional Space. *International Journal of Theoretical Physics*, 10(6):363–384, Sep 1974.

[16] Macarena Lagos et al. A general theory of linear cosmological perturbations: stability conditions, the quasistatic limit and dynamics. *Journal of Cosmology and Astroparticle Physics*, 2018(03), Mar 2018.

[17] Lucas Lombriser and Andy Taylor. Breaking a Dark Degeneracy with Gravitational Waves. *Journal of Cosmology and Astroparticle Physics*, 2016(03), Mar 2016.

[18] Lucas Lombriser, Charles Dalang, Joe Kennedy, and Andy Taylor. Inherently stable effective field theory for dark energy and modified gravity. *Journal of Cosmology and Astroparticle Physics*, 2019(01), Jan 2019.

[19] Albert Einstein. Kosmologische Betrachtungen zur allgemeinen Relativitätstheorie. *Sitzungsberichte der Königlich Preußischen Akademie der Wissenschaften (Berlin*, pages 142–152, January 1917.

[20] Christopher Ray. The cosmological constant: Einstein's greatest mistake? *Studies in History and Philosophy of Science Part A*, 21(4):589 – 604, 1990.

[21] N. Aghanim et al. Planck 2018 results. VI. Cosmological parameters.

[22] M. M. Phillips. The Absolute Magnitudes of Type IA Supernovae. , 413:L105, August 1993.

[23] A. Friedman. Über die krümmung des raumes. *Zeitschrift für Physik*, 10(1):377–386, Dec 1922.

[24] Adam G. Riess et al. Type Ia Supernova Discoveries at $z > 1$ from the Hubble Space Telescope: Evidence for Past Deceleration and Constraints on Dark Energy Evolution. *The Astrophysical Journal*, 607(2):665–687, Jun 2004.

[25] J. Guy et al. The supernova legacy survey 3-year sample: Type ia supernovae photometric distances and cosmological constraints. *Astronomy Astrophysics*, 523:A7, Nov 2010.

[26] Lawrence M Krauss, Katherine Jones-Smith, and Dragan Huterer. Dark energy, a cosmological constant, and type Ia supernovae, journal = New Journal of Physics. 9(5):141–141, may 2007.

[27] Ashutosh Tripathi, Archana Sangwan, and H.K. Jassal. Dark energy equation of state parameter and its evolution at low redshift. *Journal of Cosmology and Astroparticle Physics*, 2017(06):012–012, Jun 2017.

[28] P. de Bernardis et al. A flat Universe from high-resolution maps of the cosmic microwave background radiation. *Nature*, 404(6781):955–959, Apr 2000.

[29] A. Balbi et al. Constraints on cosmological parameters from MAXIMA-1. *The Astrophysical Journal*, 545(1):L1–L4, dec 2000.

[30] G. Hinshaw et al. Nine-Year Wilkinson Microwave Anisotropy Probe (WMAP) Observations: Cosmological Parameter Results. *The Astrophysical Journal Supplement Series*, 208(2):19, Sep 2013.

[31] Alan H. Guth. Inflationary universe: A possible solution to the horizon and flatness problems. *Phys. Rev. D*, 23:347–356, Jan 1981.

[32] A. C. Fabian. On the baryon content of the Shapley supercluster. *Monthly Notices of the Royal Astronomical Society*, 253:29P, December 1991.

[33] Raul Jimenez et al. Ages of globular clusters: a new approach. *Monthly Notices of the Royal Astronomical Society*, 282(3):926–942, Oct 1996.

[34] Megan Donahue et al. A Very Hot High-Redshift Cluster of Galaxies: More Trouble for $\Omega_0 = 1$. *The Astrophysical Journal*, 502(2):550–557, Aug 1998.

[35] Tzu-Ching Chang, Ue-Li Pen, Jeffrey B. Peterson, and Patrick McDonald. Baryon acoustic oscillation intensity mapping of dark energy. *Phys. Rev. Lett.*, 100:091303, Mar 2008.

[36] Jérôme Martin. Everything you always wanted to know about the cosmological constant problem (but were afraid to ask). *Comptes Rendus Physique*, 13(6):566 – 665, 2012. Understanding the Dark Universe.

[37] Michael Florian Wondrak. *The Cosmological Constant and Its Problems: A Review of Gravitational Aether*, pages 109–120. Springer International Publishing, Cham, 2018.

[38] Sean M. Carroll, William H. Press, and Edwin L. Turner. The Cosmological Constant. *Annual Review of Astronomy and Astrophysics*, 30(1):499–542, 1992.

[39] S.E. Rugh and H. Zinkernagel. The Quantum Vacuum and the Cosmological Constant Problem. *Studies in History and Philosophy of Science Part B: Studies in History and Philosophy of Modern Physics*, 33(4):663 – 705, 2002.

[40] H. E. S. Velten, R. F. vom Marttens, and W. Zimdahl. Aspects of the cosmological "coincidence problem". *The European Physical Journal C*, 74(11):3160, Nov 2014.

[41] Hayato Motohashi and Teruaki Suyama. Third-order equations of motion and the ostrogradsky instability. *Physical Review D*, 91, 11 2014.

[42] C. Brans and R. H. Dicke. Mach's principle and a relativistic theory of gravitation. *Phys. Rev.*, 124:925–935, Nov 1961.

[43] Bharat Ratra and P. J. E. Peebles. Cosmological consequences of a rolling homogeneous scalar field. *Phys. Rev. D*, 37:3406–3427, Jun 1988.

[44] Christos Charmousis et al. General Second-Order Scalar-Tensor Theory and Self-Tuning. *Physical Review Letters*, 108(5), Jun 2011.

[45] Sourav Bhattacharya and Sumanta Chakraborty. Constraining some Horndeski gravity theories. *Phys. Rev. D*, 95:044037, Feb 2017.

[46] Emilio Bellini et al. Constraints on deviations from CDM within Horndeski gravity. *Journal of Cosmology and Astroparticle Physics*, 2016(02), Feb 2016.

[47] Tsutomu Kobayashi. Horndeski theory and beyond: a review. *Reports on Progress in Physics*, 82(8), Jul 2019.

[48] C. Armendáriz-Picón, T. Damour, and V. Mukhanov. k-Inflation. *Physics Letters B*, 458(2-3):209–218, Jul 1999.

[49] Cédric Deffayet, Oriol Pujolàs, Ignacy Sawicki, and Alexander Vikman. Imperfect Dark Energy from Kinetic Gravity Braiding. *Journal of Cosmology and Astroparticle Physics*, 2010(10):026–026, Oct 2010.

[50] Emilio Bellini and Ignacy Sawicki. Maximal freedom at minimum cost: linear large-scale structure in general modifications of gravity. *Journal of Cosmology and Astroparticle Physics*, 2014(07), Jul 2014.

[51] Lucas Lombriser and Andy Taylor. Semi-dynamical perturbations of unified dark energy. *Journal of Cosmology and Astroparticle Physics*, 2015(11), Nov 2015.

[52] M. White and W. Hu. The Sachs-Wolfe effect. *Astronomy and Astrophysics*, 321:8–9, Oct 1996.

[53] Shadab Alam et al. The clustering of galaxies in the completed SDSS-III Baryon Oscillation Spectroscopic Survey: cosmological analysis of the DR12 galaxy sample. *Monthly Notices of the Royal Astronomical Society*, 470(3):2617–2652, Mar 2017.

[54] Yong-Seon Song and Will J Percival. Reconstructing the history of structure formation using redshift distortions. *Journal of Cosmology and Astroparticle Physics*, 2009(10):004–004, Oct 2009.

[55] Michael J. Hudson and Stephen J. Turnbull. The Growth Rate of Cosmic Structure from Peculiar Velocities at Low and High Redshifts. *The Astrophysical Journal*, 751(2):L30, may 2012.

[56] Chris Blake et al. The WiggleZ Dark Energy Survey: joint measurements of the expansion and growth history at $z < 1$. *Monthly Notices of the Royal Astronomical Society*, 425(1):405–414, Jul 2012.

[57] L. Samushia, W. J. Percival, and A. Raccanelli. Interpreting large-scale redshift-space distortion measurements. *Monthly Notices of the Royal Astronomical Society*, 420(3):2102–2119, 02 2012.

[58] Florian Beutler et al. The 6dF Galaxy Survey: $z \approx 0$ measurements of the growth rate and σ_8. *Monthly Notices of the Royal Astronomical Society*, 423(4):3430–3444, 07 2012.

[59] Rita Tojeiro et al. The clustering of galaxies in the SDSS-III Baryon Oscillation Spectroscopic Survey: measuring structure growth using passive galaxies. *Monthly Notices of the Royal Astronomical Society*, 424(3):2339–2344, 08 2012.

[60] S. de la Torre et al. The VIMOS Public Extragalactic Redshift Survey (VIPERS). *Astronomy Astrophysics*, 557:A54, Aug 2013.

[61] Chia-Hsun Chuang and Yun Wang. Modelling the anisotropic two-point galaxy correlation function on small scales and single-probe measurements of H(z), DA(z) and f(z)8(z) from the Sloan Digital Sky Survey DR7 luminous red galaxies. *Monthly Notices of the Royal Astronomical Society*, 435(1):255–262, 08 2013.

[62] Chris Blake et al. Galaxy And Mass Assembly (GAMA): improved cosmic growth measurements using multiple tracers of large-scale structure. *Monthly Notices of the Royal Astronomical Society*, 436(4):3089–3105, Oct 2013.

[63] Ariel G. Sánchez et al. The clustering of galaxies in the SDSS-III Baryon Oscillation Spectroscopic Survey: cosmological implications of the full shape of the clustering wedges in the data release 10 and 11 galaxy samples. *Monthly Notices of the Royal Astronomical Society*, 440(3):2692–2713, Apr 2014.

[64] Cullan Howlett et al. The clustering of the SDSS main galaxy sample – II. Mock galaxy catalogues and a measurement of the growth of structure from redshift space distortions at $z = 0.15$. *Monthly Notices of the Royal Astronomical Society*, 449(1):848–866, Mar 2015.

[65] Martin Feix, Adi Nusser, and Enzo Branchini. Growth Rate of Cosmological Perturbations at $z \sim 0.1$ from a New Observational Test. *Physical Review Letters*, 115(1), Jun 2015.

[66] Teppei Okumura et al. The Subaru FMOS galaxy redshift survey (FastSound). IV. New constraint on gravity theory from redshift space distortions at $z \sim 1.4$. *Publications of the Astronomical Society of Japan*, 68(3):38, Apr 2016.

[67] Chia-Hsun Chuang et al. The clustering of galaxies in the SDSS-III Baryon Oscillation Spectroscopic Survey: single-probe measurements from CMASS anisotropic galaxy clustering. *Monthly Notices of the Royal Astronomical Society*, 461(4):3781–3793, Jun 2016.

[68] Florian Beutler et al. The clustering of galaxies in the completed SDSS-III Baryon Oscillation Spectroscopic Survey: anisotropic galaxy clustering in Fourier space. *Monthly Notices of the Royal Astronomical Society*, 466(2):2242–2260, Dec 2016.

[69] Michael J. Wilson. Geometric and growth rate tests of General Relativity with recovered linear cosmological perturbations, 2016.

[70] Héctor Gil-Marín et al. The clustering of galaxies in the SDSS-III Baryon Oscillation Spectroscopic Survey: RSD measurement from the power spectrum and bispectrum of the DR12 BOSS galaxies. *Monthly Notices of the Royal Astronomical Society*, 465(2):1757–1788, Oct 2016.

[71] A. J. Hawken et al. The VIMOS Public Extragalactic Redshift Survey. *Astronomy Astrophysics*, 607:A54, Nov 2017.

[72] Dragan Huterer, Daniel L. Shafer, Daniel M. Scolnic, and Fabian Schmidt. Testing cdm at the lowest redshifts with sn ia and galaxy velocities. *Journal of Cosmology and Astroparticle Physics*, 2017(05):015–015, May 2017.

[73] S. de la Torre et al. The VIMOS Public Extragalactic Redshift Survey (VIPERS). *Astronomy Astrophysics*, 608:A44, Dec 2017.

[74] A. Pezzotta et al. The VIMOS Public Extragalactic Redshift Survey (VIPERS). *Astronomy Astrophysics*, 604:A33, Jul 2017.

[75] Cullan Howlett et al. 2MTF – VI. Measuring the velocity power spectrum. *Monthly Notices of the Royal Astronomical Society*, 471(3):3135–3151, Jun 2017.

[76] F. G. Mohammad et al. The VIMOS Public Extragalactic Redshift Survey (VIPERS). *Astronomy Astrophysics*, 610:A59, Feb 2018.

[77] Yuting Wang et al. The clustering of galaxies in the completed SDSS-III Baryon Oscillation Spectroscopic Survey: a tomographic analysis of structure growth and expansion rate from anisotropic galaxy clustering. *Monthly Notices of the Royal Astronomical Society*, 481(3):3160–3166, Sep 2018.

[78] Feng Shi et al. Mapping the Real Space Distributions of Galaxies in SDSS DR7. II. Measuring the Growth Rate, Clustering Amplitude of Matter, and Biases of Galaxies at Redshift 0.1. *The Astrophysical Journal*, 861(2):137, Jul 2018.

[79] Héctor Gil-Marín et al. The clustering of the SDSS-IV extended Baryon Oscillation Spectroscopic Survey DR14 quasar sample: structure growth rate measurement from the anisotropic quasar power spectrum in the redshift range $0.8 < z < 2.2$. *Monthly Notices of the Royal Astronomical Society*, 477(2):1604–1638, Feb 2018.

[80] Jiamin Hou et al. The clustering of the SDSS-IV extended Baryon Oscillation Spectroscopic Survey DR14 quasar sample: anisotropic clustering analysis in configuration space. *Monthly Notices of the Royal Astronomical Society*, 480(2):2521–2534, Jul 2018.

[81] Gong-Bo Zhao et al. The clustering of the SDSS-IV extended Baryon Oscillation Spectroscopic Survey DR14 quasar sample: a tomographic measurement of cosmic structure growth and expansion rate based on optimal redshift weights. *Monthly Notices of the Royal Astronomical Society*, 482(3):3497–3513, Oct 2018.

[82] Lavrentios Kazantzidis and Leandros Perivolaropoulos. Evolution of the $f\sigma_8$ tension with the planck15/λcdm determination and implications for modified gravity theories. *Physical Review D*, 97(10), May 2018.

[83] Euclid Consortium. `https://www.euclid-ec.org`. Accessed: 2020-04-01.

Appendices

Note — Appendices are provided for completeness only and any content included in them will be disregarded for the purposes of assessment.

A Derivations

This section contains derivations that are omitted in the body of the report.

A.1 Sound Speed Equation

A.1.1 Hubble Factor Term

Solving H'/H (second to last term of Eq. 27). Starting with,

$$H = H_0 \left(\Omega_m a^{-3} + \Omega_v\right)^{\frac{1}{2}}, \tag{46}$$

$$H' = H_0 \frac{d}{d\ln a} \left(\Omega_m a^{-3} + \Omega_v\right)^{\frac{1}{2}} = \frac{H_0}{2} \left(\Omega_m a^{-3} + \Omega_v\right)^{-\frac{1}{2}} \left(-3\Omega_m a^{-3}\right), \tag{47}$$

$$\frac{H'}{H} = -\frac{3}{2} \frac{\Omega_m a^{-3}}{\Omega_m a^{-3} + \Omega_v} \equiv -\frac{3}{2}\Omega_m(a). \tag{48}$$

A.1.2 Friedmann Term

Solving $\rho_m/(2H^2M^2)$ (last term of Eq. 27). Starting with the flat present day Friedmann equation,

$$H_0^2 = \frac{8\pi G}{3}\rho_0, \tag{49}$$

$$\Omega_m H^2 = \frac{8\pi G}{3}\rho_{m,0}, \tag{50}$$

with $M^2 \equiv \frac{1}{8\pi G}$,

$$\rho_{m,0} = 3H_0^2 M^2 \Omega_m. \tag{51}$$

So from,

$$\frac{\rho_m}{2H^2M^2} = \frac{\rho_{m,0}}{2H^2M^2}a^{-3} = \frac{3H_0^2\Omega_m a^{-3}}{2H^2}. \tag{52}$$

Finally, as $H^2 = H_0^2\left(\Omega_m a^{-3} + \Omega_v\right)$,

$$\frac{\rho_m}{2H^2M^2} = \frac{3}{2}\frac{\Omega_m a^{-3}}{\Omega_m a^{-3} + \Omega_v} \equiv \frac{3}{2}\Omega_m(a) \tag{53}$$

B Additional Plots

B.1 Potentials with Varying Present-Day Planck Mass

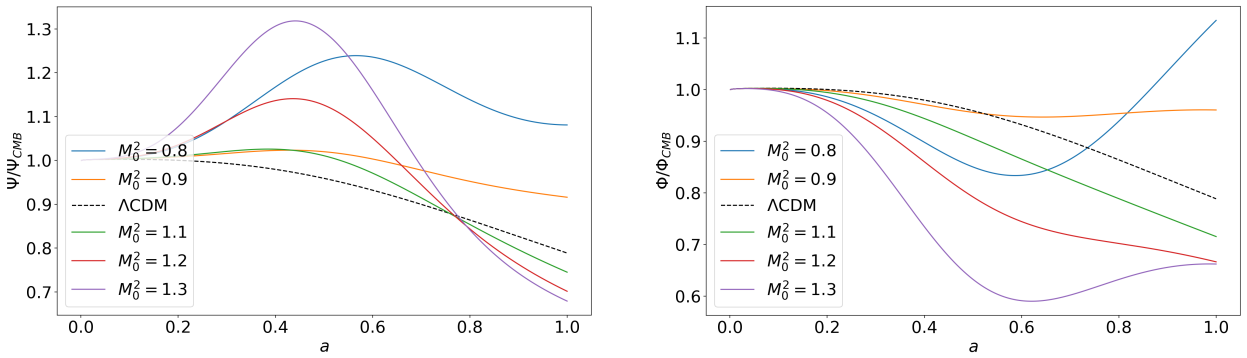

Figure 8. Left: Evolution of Ψ with varying M^2 at constant $\xi_0 = 0.2$. This conveys that the enhancement of μ at early times is proportional to the M^2 deviation from ΛCDM. Right: Evolution of Φ in the same regime. This comparable to the evolution of Ψ except the early enhancement of the potential is replaced by a suppression. This due to the formalism of γ which is small at early times in this regime.